Article

Neuron

Genetic Differences in the Immediate Transcriptome Response to Stress Predict Risk-Related Brain Function and Psychiatric Disorders

Highlights

- SNPs in long-range enhancers alter the transcriptional response of GR target genes
- These functional SNPs predict risk for psychiatric but not other medical disorders
- These variants are associated with differential neural circuit responses to threat
- GR transcripts are strongly co-expressed and regulated in the brain of animal models

Authors

Janine Arloth, Ryan Bogdan, ..., Ahmad R. Hariri, Elisabeth B. Binder

Correspondence

binder@psych.mpg.de

In Brief

Using a stimulated eQTL approach, Arloth et al. show that common genetic variants that alter the initial transcriptome response to stress hormone receptor activation also cumulatively increase the risk for stress-related psychiatric disorders and predict a threat response from the amygdala.

Accession Numbers

GSE46743

Arloth et al., 2015, Neuron *86*, 1189–1202
June 3, 2015 ©2015 The Authors
http://dx.doi.org/10.1016/j.neuron.2015.05.034

CellPress

Neuron
Article

Genetic Differences in the Immediate Transcriptome Response to Stress Predict Risk-Related Brain Function and Psychiatric Disorders

Janine Arloth,[1] Ryan Bogdan,[3] Peter Weber,[1] Goar Frishman,[4] Andreas Menke,[1] Klaus V. Wagner,[10] Georgia Balsevich,[10] Mathias V. Schmidt,[10] Nazanin Karbalai,[1] Darina Czamara,[1] Andre Altmann,[9] Dietrich Trümbach,[4] Wolfgang Wurst,[1,4,6,7] Divya Mehta,[1] Manfred Uhr,[1] Torsten Klengel,[1] Angelika Erhardt,[1] Caitlin E. Carey,[3] Emily Drabant Conley,[5] Major Depressive Disorder Working Group of the Psychiatric Genomics Consortium (PGC), Andreas Ruepp,[4] Bertram Müller-Myhsok,[1] Ahmad R. Hariri,[2] and Elisabeth B. Binder[1,8,*]
[1]Department of Translational Research in Psychiatry, Max Planck Institute of Psychiatry, Munich 80804, Germany
[2]Department of Psychology and Neuroscience, Institute for Genome Sciences and Policy, Duke University, Durham, NC 27708, USA
[3]Department of Psychology, Washington University in St. Louis, St. Louis, MO 63130, USA
[4]Helmholtz Zentrum München - German Research Center for Environmental Health, Neuherberg 85764, Germany
[5]23andMe, Mountain View, CA 94043, USA
[6]Technische Universität München, c/o Helmholtz Zentrum München, German Research Centre for Environmental Health, Institute of Developmental Genetics, Neuherberg 85764, Germany
[7]Deutsches Zentrum für Neurodegenerative Erkrankungen e. V. (DZNE), Site Munich, Munich 80336, Germany
[8]Department of Psychiatry and Behavioral Sciences, Emory University School of Medicine, Atlanta, GA 30329, USA
[9]Department of Neurology and Neurological Sciences, School of Medicine, Stanford University, Palo Alto, CA 94304, USA
[10]Department of Stress Neurobiology and Neurogenetics, Max Planck Institute of Psychiatry, Munich 80804, Germany
*Correspondence: binder@psych.mpg.de
http://dx.doi.org/10.1016/j.neuron.2015.05.034
This is an open access article under the CC BY-NC-ND license (http://creativecommons.org/licenses/by-nc-nd/4.0/).

SUMMARY

Depression risk is exacerbated by genetic factors and stress exposure; however, the biological mechanisms through which these factors interact to confer depression risk are poorly understood. One putative biological mechanism implicates variability in the ability of cortisol, released in response to stress, to trigger a cascade of adaptive genomic and non-genomic processes through glucocorticoid receptor (GR) activation. Here, we demonstrate that common genetic variants in long-range enhancer elements modulate the immediate transcriptional response to GR activation in human blood cells. These functional genetic variants increase risk for depression and co-heritable psychiatric disorders. Moreover, these risk variants are associated with inappropriate amygdala reactivity, a transdiagnostic psychiatric endophenotype and an important stress hormone response trigger. Network modeling and animal experiments suggest that these genetic differences in GR-induced transcriptional activation may mediate the risk for depression and other psychiatric disorders by altering a network of functionally related stress-sensitive genes in blood and brain.

INTRODUCTION

Major depressive disorder (MDD) has a lifetime prevalence of up to 17% (Kessler et al., 2005), resulting in one of the highest global burden of disease ratings by the World Health Organization (Ustün et al., 2004). Despite its prevalence and impact, the etiological and pathophysiological mechanisms underlying MDD are poorly understood, resulting in sub-optimal treatments with high rates of recurrence and treatment resistance (Warden et al., 2007). Family, twin, and population studies point to both genetic as well as environmental risk factors for depression. Genetic factors contribute up to 40% of the risk and are complemented largely by individual-specific environmental exposure to adverse life events (Kendler et al., 2006). Both sensitivity and resilience to the long-term effects of exposure to adverse life events may be modulated by genetic variation (Kendler, 2013).

Stress results in activation of the stress hormone system, which culminates in the activation of glucocorticoid receptors (GRs) by cortisol. The GR is a nuclear hormone receptor, and upon activation it translocates from the cytoplasm to the nucleus, where it binds to glucocorticoid response elements (GREs) and regulates gene expression (McKay and Cidlowski, 1999; Phuc Le et al., 2005). Activation of this receptor not only initiates adaptive physiological changes in the body to confront an imminent threat, but also facilitates the termination of these changes once the threat has been overcome. Thus, genetically driven variability in GR regulation of the stress hormone response may functionally interact with environmental risk factors, thereby producing individual differences in risk for MDD.

Consistent with this model, dysfunction of GR-mediated negative feedback has been reported in MDD (de Kloet et al., 2005) as well as in individuals exposed to early adversity (Heim and Binder, 2012; Wilkinson and Goodyer, 2011), one of the strongest risk factors for the development of MDD. Moreover, genetic variation in pathways regulating GR signaling has been linked with MDD risk (van Rossum et al., 2006). Here, we show that

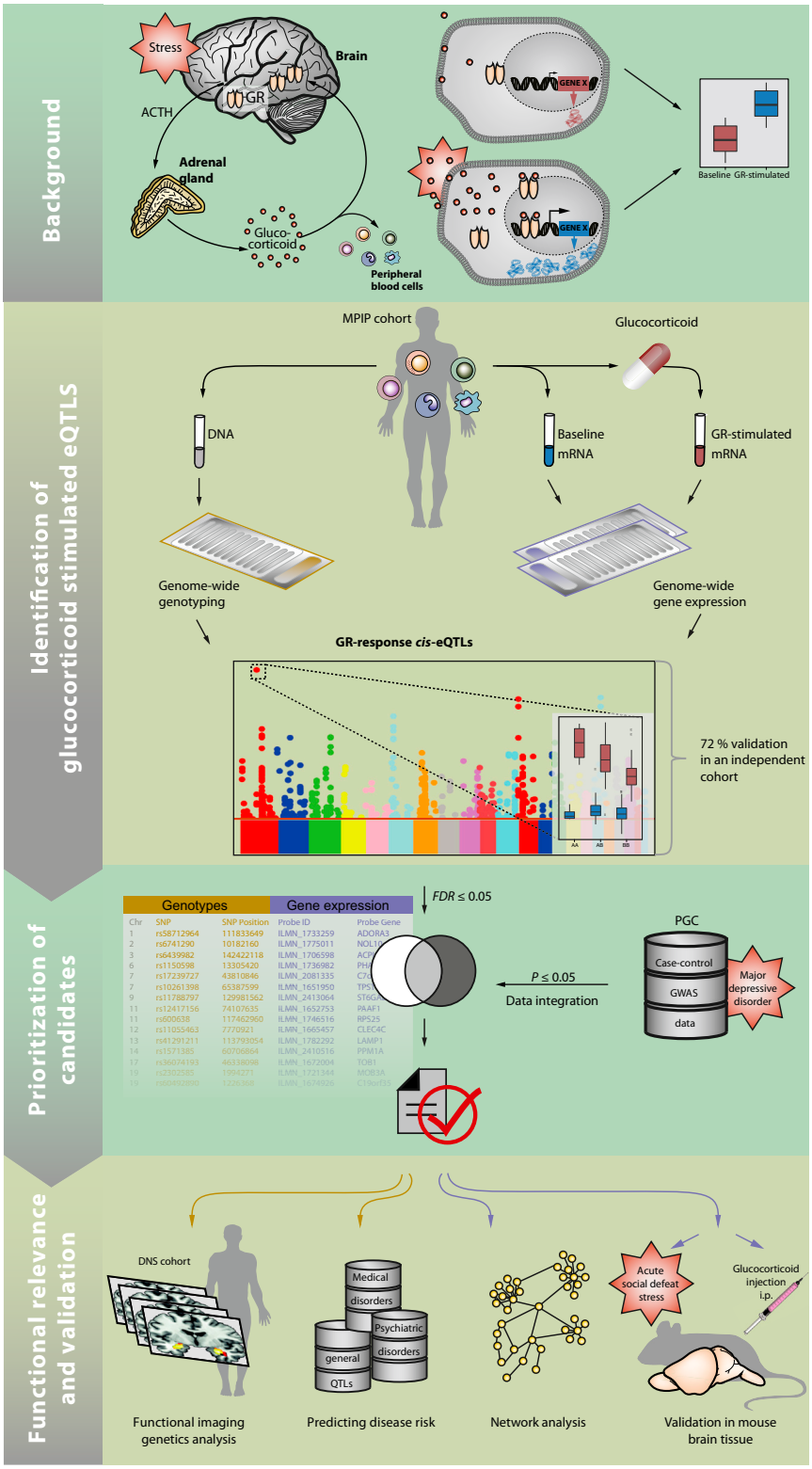

Figure 1. Summary Figure Illustrating the Sequence of Experiments and Analyses Applied in This Study

The main hypothesis tested in this study is that common genetic variants that alter the short-term transcriptional response to GR activation also alter the risk for stress-related psychiatric disorders and related neural endophenotypes.

common genetic variants that modulate the initial transcriptional response to GR activation increase the risk for MDD as well as other psychiatric disorders. Gene network modeling and animal experiments suggest that these genetic differences in the transcriptional response to GR activation may mediate risk for depression and other psychiatric disorders by altering a network of co-expressed genes that are responsive to stress and glucocorticoids in the brain. In addition, these genetic variants shape the response of the amygdala, which is itself an important trigger of the stress hormone response and a functional neural phenotype implicated in the etiology and pathophysiology of depression and other forms of psychopathology (Jankord and Herman, 2008; Phillips et al., 2003). The main hypotheses and the experimental approach are summarized in Figure 1.

RESULTS

Genetic Regulation of GR-Stimulated Gene Expression

We first identified genetic variants that alter GR-stimulated gene expression changes by adopting a stimulated expression quantitative trait locus (eQTL) approach (Figure 2A). Gene expression profiles in peripheral blood cells from 160 male individuals of the Max-Planck Institute of Psychiatry (MPIP) cohort (91 cases and 69 controls, see Experimental Procedures) were obtained at baseline and 3 hr after stimulation with the selective GR agonist dexamethasone (Figure S1A) and combined with genome-wide SNP data. All individuals showed a strong endocrine response to dexamethasone (Cortisol: $F_{1,159}$ = 43.93, p = 5.02 × 10^{-10} and ACTH: $F_{1,158}$ = 37.96, p = 5.76 × 10^{-9}; Figures S1B and S1C). After quality control, 4,447 gene expression probes that exhibited strong regulation following dexamethasone administration (absolute fold change in gene expression from baseline to 3 hr post-dexamethasone ≥ 1.3 in at least 20% of all samples) were combined with genotype data of ~2 million imputed SNPs (see Experimental Procedures). Using the log fold change in gene

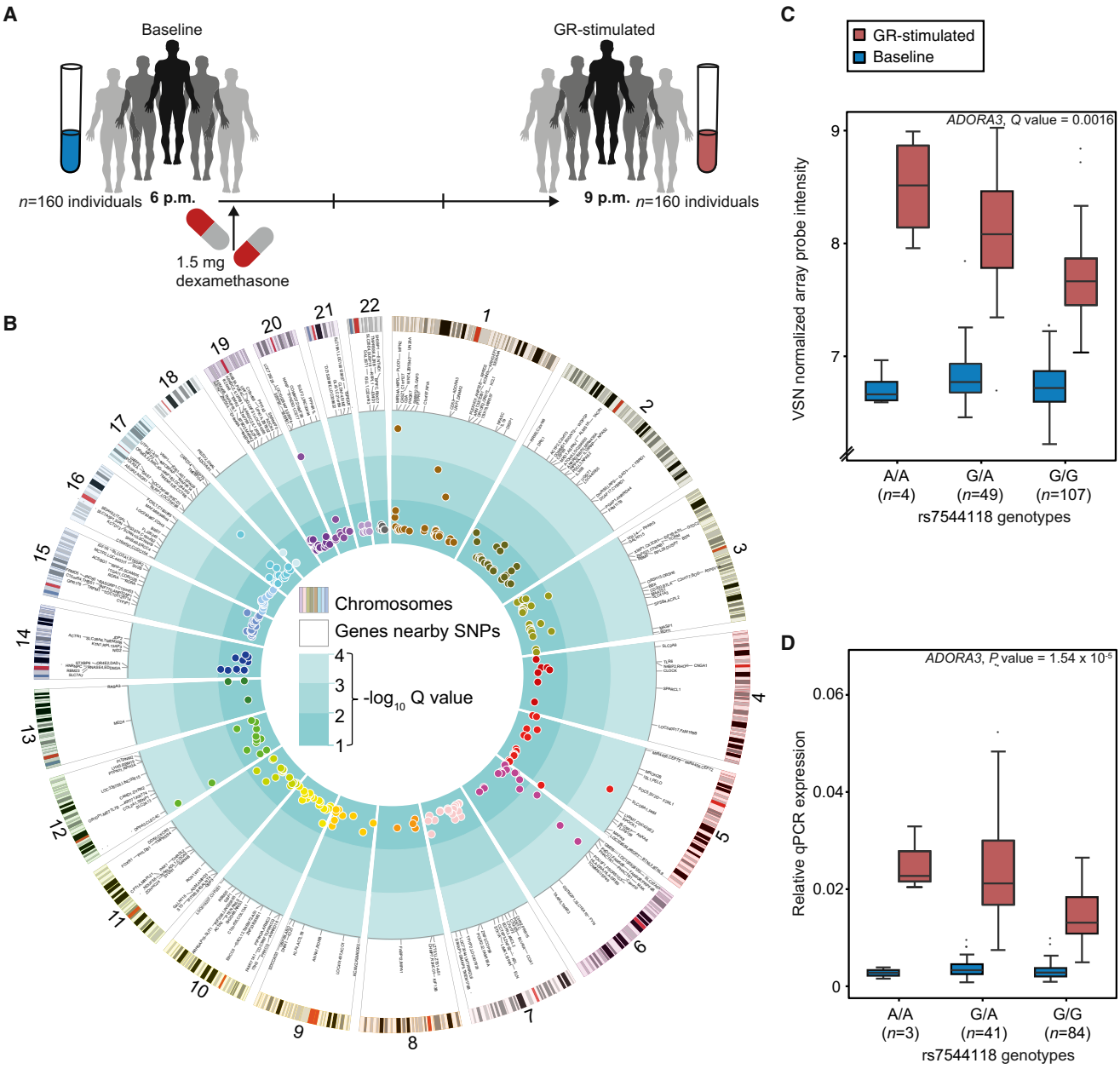

Figure 2. GR-Response-Modulating *cis*-eQTLs

(A) Study design for GR-stimulated gene expression in whole blood of 160 male individuals from the Max Planck Institute of Psychiatry cohort.

(B) Circularized Manhattan plot displaying *cis*-associations for GR-response eQTL bins (n = 320) and their respective significance ($-\log_{10}$ Q values). Displayed from the outer to the inner circle are the number of chromosomes, the ideograms for the human karyotype (hg18), genes nearby eSNPs, and Manhattan plots for the eQTL bins that survived correction for multiple testing.

(C and D) Boxplots of human gene expression values for *ADORA3*, which is an example of a significant GR-response eQTL. Expression levels are stratified based on the eSNP genotypes for *ADORA3*. Baseline (6 p.m.) measures are displayed in blue and GR-stimulated measures (9 p.m.) in red. Microarrays data are displayed in (C) and their qPCR validation in (D). Q value in (C) is derived from GR-response *cis*-eQTL analysis and the p value in (D) from the qPCR linear regression model.

expression standardized to baseline values as the outcome and restricting the analysis to a ± 1 Mb *cis*-region around each probe, we found that 3,820 GR-response-modulating *cis*-eQTLs (GR-response eQTLs) remained significant after accounting for disease status, age, and BMI and correction for multiple testing (see Experimental Procedures). These comprised 297 unique array probes and 3,662 unique SNPs. The 3,662 unique GR-response *cis*-expression SNPs (eSNPs) can be summarized in terms of independent tag SNPs into 296 uncorrelated GR-response *cis*-eSNP bins, i.e., sets of SNPs in linkage

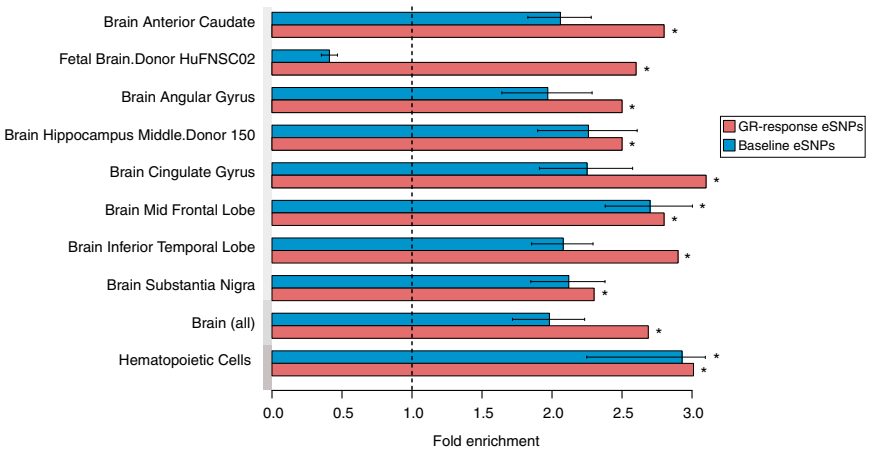

Figure 3. GR-Response eSNPs Are Enriched in Enhancer Regions in Multiple Tissues

Bar graph illustrating the enrichment of GR-response eSNPs for enhancers in multiple tissues from the Roadmap Epigenome Project, including brain tissue. The x axis shows the fold enrichment and the y axis all brain enhancers all well as the mean fold enrichment among all hematopoietic cells (see Figure S2) and brain enhancers. The fold enrichment for GR-response eSNPs is illustrated in red and for the permuted baseline eSNPs in blue. Only the GR-response eSNP enrichment, which passes a Bonferroni corrected significance threshold (corrected for the number of all tested tissues or cells, n = 62) is illustrated. * $p \leq 0.05$, obtained by binomial enrichment test and Bonferroni correction, error bars ± SD.

disequilibrium (LD; see Experimental Procedures). We defined the tag eSNP as the eSNP showing the highest association per bin (lowest Q value). These 296 GR-response *cis*-eSNP bins correspond to 320 GR-response *cis*-eQTL bins, i.e., *cis*-eSNP bin-probe combinations, as one *cis*-eSNP bin can be associated with the regulation of more than one transcript and vice versa. These GR-response *cis*-eQTL bins are listed in Table S1 and illustrated in Figures 2B–2D. Including dexamethasone serum levels or the blood cell count as covariate did not change the results, excluding any confounding effects of individual differences in dexamethasone concentration and cellular composition (see Supplemental Information).

To assess the robustness of these GR-response eQTLs, we validated them in an independent sample of n = 58 (see Experimental Procedures) by performing a sample size-weighted *Z* score meta-analysis across both samples. In this analysis, 72% of the GR-response eQTLs could be validated, i.e., showed a meta-analysis p value equal to or more significant than in the discovery sample alone (see Experimental Procedures). This method accounts for the small size of the validation sample and suggests the robustness of most of the GR-response eQTLs.

Characterization of GR-Response eSNPs

To better understand the properties of these GR-response eQTLs, we first mapped the GR-eSNPs (n = 3,662 SNPs) to GR binding regions as defined by ChIP-seq peaks in lymphoblastoid cell line (LCL) GM12878 (see Experimental Procedures). We observed a significant enrichment of GR-response eSNPs in GR binding sites as compared to random SNPs (fold enrichment = 2.4, permutation-based FDR $\leq$ 0.001).

Next, we mapped the distance of the 320 GR-response eQTL bins to the genomic location of the probe sequence of the respective regulated transcript (utilizing the closest SNP within a bin) and compared this to the probe distance for baseline *cis*-eQTL bins, i.e., the eSNP-probe combinations that showed a significant association of the genotype with transcription levels at baseline (see Supplemental Information). The GR-response eSNP bin-to-probe distance (mean = 406 kb, standard deviation [SD] = 303 kb, n = 320 bins) was significantly longer (Wilcoxon p value = 1.03×10^{-50}) than baseline eSNP bin-to-probe distance (mean = 149 kb, SD = 232 kb, n = 1,148 bins; Supplemental Information). This suggests that GR stimulation is associated with significantly more long-range transcriptional regulation than baseline gene expression and that distinct regulatory elements may be involved in baseline versus GR-stimulated gene transcription.

To determine the regulatory potential of GR-response eSNPs, we investigated whether they are enriched within enhancer regions as defined by the Roadmap Epigenome Project (Kundaje et al., 2015) (see Experimental Procedures). GR-response tag eSNPs were significantly enriched within enhancers in 62 different tissues, including blood cells, but also non-hematopoietic tissue such as brain (see Figure S2). When testing baseline tag eSNPs, we only observed an enrichment in enhancers in 54% of these 62 tissues. Whether combined enrichment of both GR-response tag eSNPs and baseline tag eSNPs was observed seemed to be tissue specific (see Figure S2). In fact, GR-response eSNPs were more enriched in brain enhancers than baseline eSNPs, i.e., only one of the eight brain enhancers significantly enriched with GR-response eSNPs also displayed a significant enrichment for baseline eSNPs (see Figure 3). In contrast, we observed equal enrichment for GR-response as well as baseline eSNPs in primary hematopoietic tissues (see Figure S2). These results further support the viewpoint that GR-response eSNPs affect different transcriptional regulators than baseline eSNPs and suggest possible cross-tissue effects of these SNPs.

To evaluate whether the long-range regulation of GR-response eQTLs may be associated with long-range physical chromatin interaction, we compared our data with that from a chromatin interaction analysis with paired-end tag sequencing (ChIA-PET) generated by ENCODE (ENCODE Project Consortium, 2011) in the leukemia cell line K562. For this, we examined whether regions containing the GR-response eSNP bin and the corresponding probe gene overlap with physically interacting ChIA-PET tags (see Experimental Procedures). Twenty-five percent of the GR-response eSNP bin-probe gene combinations overlapped with chromatin interaction signals. This was significantly greater than 1,000 equally sized sets of randomly distributed GR-response eSNP bin, especially when restricting the analysis to more long-range eSNP bin-probe gene pairs with distances > 100 kb (fold enrichment$_{>100kb}$ = 1.57, permutation-based FDR$_{>100kb}$ = 0.007; see Experimental Procedures). To

validate these long-range chromatin interactions, we used a chromatin conformation capture (3C) assay to confirm a physical interaction between the eSNP bin regions of the GR-response eSNP tag rs1379868 in the *NRTN* locus and the corresponding GR-stimulated transcript *LONP1* (see Figures 4A and 4B), which is over 130 kb upstream. This eSNP bin includes a GR binding site and ChIA-PET tags (see Figure 4C), which interact with the transcription start site of the *LONP1* gene. The 3C assay confirmed an increased chromatin interaction ($p = 3.35 \times 10^{-23}$, $\chi^2 = 115.15$ at baseline) of the eSNP bin with the TSS of the *LONP1* gene (P4 in Figures 4C and 4D) in five LCLs. The average interaction frequency of these two sites was higher following stimulation with the GR-agonist dexamethasone (4.83 versus 5.65). These results suggest that long-range regulation of GR-response eQTLs could be mediated by direct chromatin interaction of enhancer regions with the respective transcription start sites.

GR-Response eSNPs Are Enriched in Loci Nominally Associated with MDD and Other Psychiatric Disorders as well as in Genome-wide Significant Schizophrenia Loci

Besides their functional characterization, an important question was to assess whether the genetic variants that alter the immediate transcriptional response to GR activation (GR-response eSNPs) would also be associated with risk for stress-related psychiatric disorder. To assess this, we first tested whether our GR-response eSNPs were overrepresented among SNPs associated with MDD in the genome-wide association study (GWAS) results of the Psychiatric Genomics Consortium (PGC), which includes approximately 9,000 cases and the same number of controls (Ripke et al., 2013). Among nominally associated loci with MDD (at meta-analysis p value ≤ 0.05), 282 SNPs also represent a GR-response eSNP. Permutation analysis (see Experimental Procedures) predicted an expected mean overlap of 210 SNPs from 1,000 randomly selected SNP sets (fold enrichment = 1.34, permutation-based FDR < 0.001; Figure 5A). We next investigated whether GR-response eSNPs were also enriched over baseline eSNPs, as SNPs associated with transcriptional changes have been shown to be more enriched in GWASs in general (Roussos et al., 2014). Again the mean overlap for 1,000 permuted baseline *cis*-eSNP sets (218 SNPs) was significantly lower than the actual overlap of GR-response eSNPs (fold enrichment = 1.29, permutation-based FDR < 0.001; Figure 5A). These enrichments remain significant when using only the tag eSNPs (n = 285) to control for possible confounding due to linkage disequilibrium (LD) structure (fold enrichment = 1.31, permutation-based FDR = 0.082).

The 282 GR-response eSNPs that overlap with MDD-associated SNPs correspond to 23 unique eSNP bins (reflecting 26 eQTL bins) that regulate 25 unique transcripts (Table S2). We call these 23 eSNP bins "MDD-related GR eSNP bins" in the remainder of the manuscript to refer to GR-response eSNPs that also show a nominal association with MDD.

Validation of Enrichment and Extension to Other Psychiatric Disorders

We next examined whether these MDD-related GR eSNPs would also be associated with MDD in an independent sample. For this we constructed a genetic risk profile score (GRPS) using the tagging SNPs of the 23 MDD-related GR eSNP bins for each individual in an independent validation sample of 1,005 MDD cases and 478 controls (Table S3; see also Experimental Procedures). We found these GRPSs to be significantly associated with MDD and that individuals with higher GRPSs were overrepresented in the case group ($Z = 3.76$, $p = 0.00017$; Figure 5B). This GRPS explains about 2.6% of the total variance for MDD in this sample, and the association of these MDD-related GR eSNP GRPSs was more significant than GRPSs constructed from 1,000 randomly generated SNP profiles (permutation-based FDR = 0.008; see Experimental Procedures).

As exposure to stressful life events is a strong risk factor not only for MDD but also for other psychiatric disorders, including bipolar disorder (BPD) and schizophrenia (SCZ) (Dohrenwend and Egri, 1981; Kendler and Karkowski-Shuman, 1997), we tested whether the GR-response eSNPs were also overrepresented among SNPs associated with other psychiatric disorders utilizing meta-analysis data from the PGC. Using this approach, we tested for for significant GR-response eSNP enrichment compared to 1,000 randomly generated baseline eSNP sets in the PGC for four additional psychiatric disorders and the cross-disorders analysis including also MDD (see Table 1). In the latest multi-stage SCZ GWAS, which includes up to 36,989 cases and 113,075 controls (Schizophrenia Working Group of the Psychiatric Genomics Consortium, 2014), we detected a significant enrichment of GR-response eSNPs compared to baseline eSNPs with SNPs associated with SCZ at $p \leq 0.05$ (fold enrichment 1.29, permutation-based FDR ≤ 0.001). When we limited the enrichment analysis to genome-wide significant SCZ loci, we detected 134 GR-response eSNPs that overlapped SNPs associated with SCZ at $p \leq 5 \times 10^{-8}$. This corresponds to a 10-fold enrichment over baseline eSNPs and is 7.75-fold higher than for nominally associated SCZ SNPs (see Table 1). A significant negative enrichment was identified for loci associated with attention deficit-hyperactivity disorder (permutation-based FDR ≤ 0.012; ADHD; 840 cases and 1,947 trio cases) and autism spectrum disorder (ASD; permutation-based FDR ≤ 0.001; 161 cases and 4,788 trio cases) but not BPD (see Table 1).

To test whether these enrichments of GR-response eSNPs as compared to baseline eSNPs are specific to psychiatric disorders, we mapped these variants to GWAS for rheumatoid arthritis, Crohn's disease, and height but found no enrichment more than 1.06-fold (see Table 1). These analyses suggest that GR-response eSNPs are unrelated to these medical disorders or general quantitative traits but specifically contribute to the risk for MDD and SCZ.

Functional Relevance of Transcripts Regulated by MDD-Related GR eSNPs

Gene Network Analysis of MDD-Related GR Genes

Next, we investigated whether the probe genes (n = 24), regulated by the MDD-related GR eSNPs, are part of specific pathways that may be relevant for the pathophysiology of psychiatric disorders. Using the GeneMANIA tool (Montojo et al., 2014), we were able to generate a gene network containing 23 of the 24 MDD-related GR genes (see Figure 6A and Experimental Procedures). Within this network, the type of interactions between the

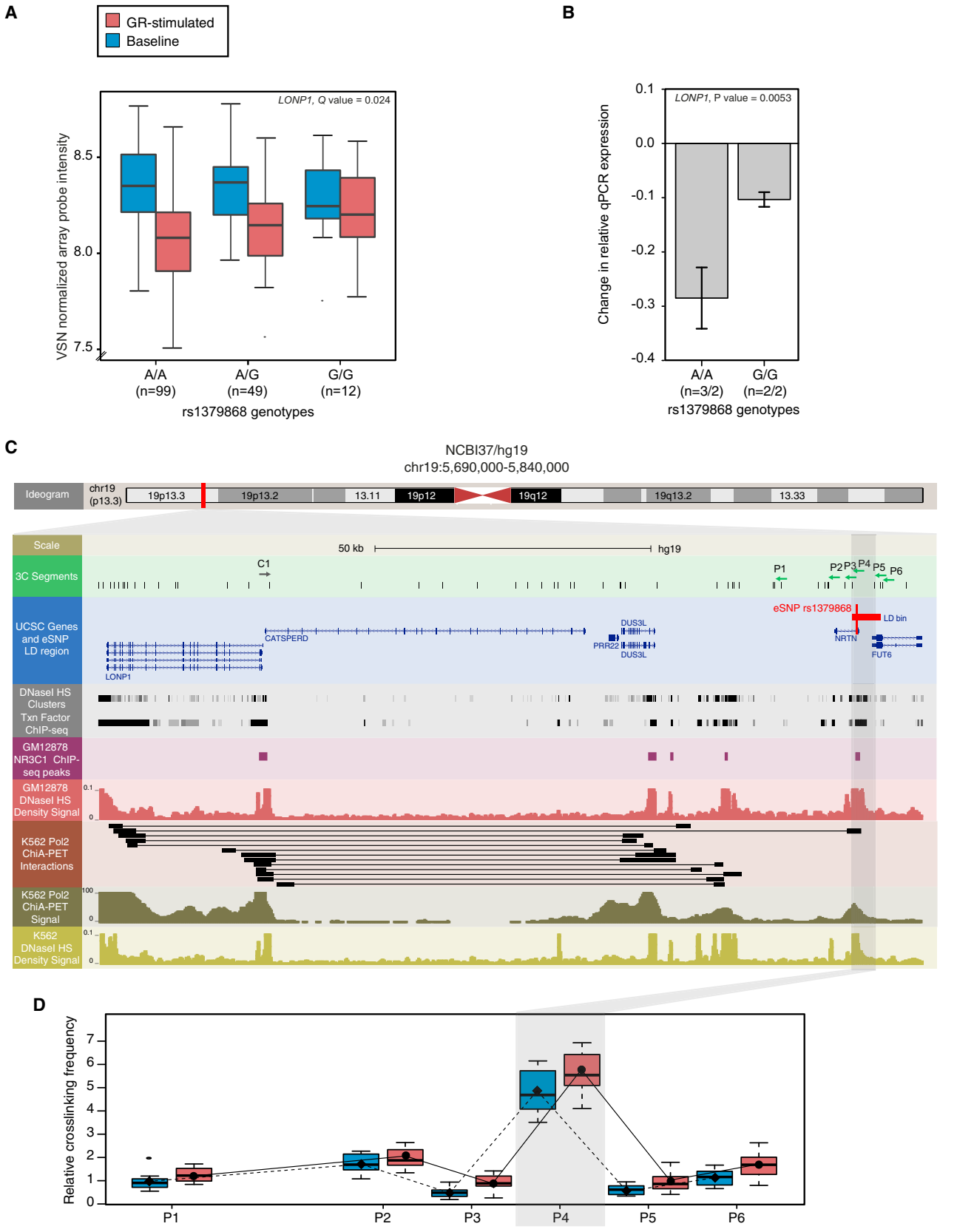

(legend on next page)

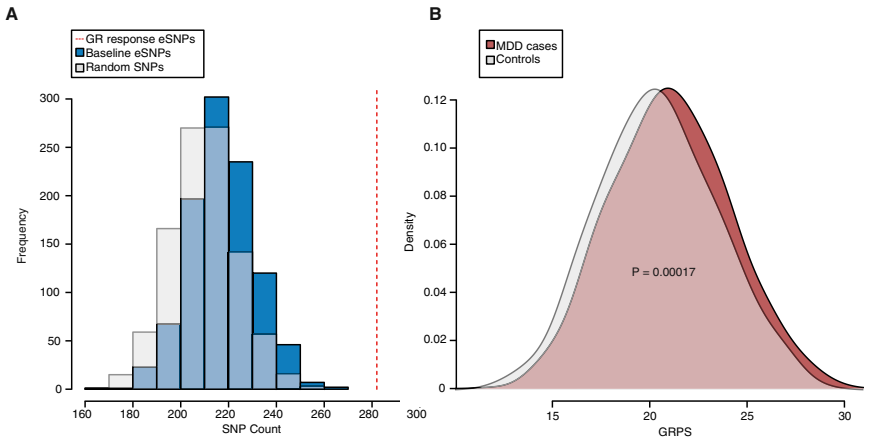

Figure 5. GR-Response eSNPs Are Enriched among Variants Associated with MDD

(A) The dotted red line shows the enriched number of GR-response eSNPs that overlap with SNPs in our meta-analysis for MDD (= MDD-related GR eSNPs; 8,864 cases and 8,982 controls). The distribution of the observed overlap for sets of 1,000 random SNPs (gray) and 1,000 random baseline eSNPs (blue) are represented as histograms (null distributions). Both permuted data sets never reached the same overlap with MDD-associated SNPs as the GR-response eSNPs.

(B) The distribution of the MDD-related GR eSNP genetic risk profile scores (GRPSs) for an independent sample of MDD cases (n = 1,005 cases; red) and controls (n = 478; gray) are represented as density plots. Individuals with MDD display higher GRPSs (p = 0.00017). p value by logistic regression model.

MDD-related GR genes that were most enriched were: co-expression (1.21 times the number expected when using other GR-stimulated transcript sets), co-localization (genes are expressed in the same tissue or proteins are found in the same location; fold enrichment = 1.21), and shared protein domains (fold enrichment = 3.77). Several genes, e.g., *FTH1*, *CCT7*, *RPS2*, *IMPDH2*, and *PELI1*, presented more than ten interactions. Additional co-expression analysis identified that the MDD-related GR genes are more tightly co-regulated in blood than in 1,000 sets of randomly chosen transcripts selected from all GR-responsive transcripts (fold enrichment = 1.04, permutation-based FDR = 0.078). These data provide support that the MDD-related GR genes functionally interact to perform an orchestrated function, i.e., they are coordinated in their transcriptional response to GR activation or stress. A limited network analysis through manually curated interactions from the scientific literature (Lechner et al., 2012) revealed that these genes show associations with MDD, SCZ, BPD, neurodevelopmental disorders, posttraumatic stress disorder, and response to antidepressant treatment in independent datasets (see Figure S3). In addition, they seem predominantly involved in pathways associated with ubiquitination and proteasome degradation and the inflammatory response, systems that have been implicated in the pathophysiology of MDD and SCZ, as well as in stress-related changes in synaptic plasticity (Miller et al., 2009; Schizophrenia Working Group of the Psychiatric Genomics Consortium, 2014; Tai and Schuman, 2008).

Convergent Functional Genomics: Integrating Human MDD-Related GR Genes with Relevant Mouse Models

To establish whether the transcripts regulated by acute GR activation in blood are also regulated in the brain within a similar time frame, we investigated whether the orthologs of the 24 MDD-related GR transcripts were differentially regulated in mouse blood and brain (prefrontal cortex [PFC], hippocampus [HC], and amygdala [AM]) 4 hr following dexamethasone administration (10 mg/kg dexamethasone i.p.). In this experiment, 17 of the 24 genes had a mouse orthologous gene, and 16 were expressed above microarray detection threshold. One-third of the genes showed significant changes at FDR $\leq$ 0.1 and 53.3% at p $\leq$ 0.05 in one or more of the investigated brain regions. Over 86% of the genes were significantly regulated (FDR $\leq$ 0.1) in mouse blood (see Figure 6B left panel).

In order to extend these results from pharmacologic GR agonism, we further evaluated whether acute social defeat stress, which is commonly used to induce depressive-like behavior, differentially regulates these same 24 MDD-related genes in mice. In this experiment, 17 orthologous genes were analyzed in blood, PFC, AM, and HC samples 4 hr after exposure to an aggressive resident mouse with short attack latency (Wagner et al., 2013). Here, three (*MKNK2*, *SLCO3A1*, and *OCIAD2*) of the five genes that were significantly differently regulated after dexamethasone stimulation were also significantly regulated following social defeat (FDR $\leq$ 0.1) in in one or more of the analyzed brain regions (see Figure 6B right panel). This suggests

Figure 4. Long-Range Chromatin Interaction of GR-Response eQTLs

(A) Long-range chromatin interaction as exemplified by the eSNP region containing the *NRTN* locus (chr10: 5,690,000–5,840,000; hg19) was confirmed by 3C in five lymphoblastoid cell lines (LCLs) each, homozygous for the two opposite SNP alleles, both in the presence and absence of dexamethasone. A SNP in the *NRTN* locus (rs1379868) affects the differentially regulated gene expression of *LONP1* in human whole blood cells (based on GR-response eQTL analysis). Baseline (6 p.m.) measures are displayed in blue and GR-stimulated measures (9 p.m.) in red.

(B) SNP effect on GR-dependent gene transcription was validated by qPCR in the LCLs used for the 3C assay.

(C) Characterization of the eSNP locus. Top panel, ideogram for chromosome 19 (p13.3). A red box isolates the region shown (enlarged) in the bottom panel. Bottom panel: 3C-primers (green track) were designed at the *LONP1* TSS (C1, anchor) and multiple regions (P1–P6) in and around the eSNP bin. The eSNP bin includes a GR binding site in blood cells (pink track). ChIA-PET tags from the leukemia cell line (brown and green tracks) validate a direct chromatin interaction between the *NRTN* eSNP locus and the regulated gene LONP1. The paired ChIA-PET tags coincide with DNaseI hypersensitivity sites in the leukemia cell line (red track) and blood cells (yellow track).

(D) Chromatin conformation capture interaction data. A 3C physical interaction between the *LONP1* TSS and eSNP bin (P4), emphasized by a gray box, was found in the 3C libraries made from LCLs ($p = 3.35 \times 10^{-23}$, $\chi^2 = 115.15$) with a stronger interaction following stimulation with the GR-agonist ($p = 0.06$, $\chi^2 = 3.35$). Q values in (A) are derived from GR-response *cis*-eQTL analysis, and p values in (B) and (D) are derived from linear mixed model; error bars ± SD.

Table 1. Proportion of GR-Response eSNPs Overlapping with GWAS SNPs with Nominal Significance

	GR-Response eSNPs	Random SNPs			Fold	Baseline eSNPs			Fold
	Count	Mean count[a]	Range	FDR	enrichment	Mean count[a]	Range	FDR	enrichment
CDA	115	86.5 ± 8.99 SD	61–119	0.001	1.33	102.03 ± 8.57 SD	71–130	0.066	1.13
BPD	91	70.36 ± 8.34 SD	44–100	0.009	1.29	86.18 ± 8.2 SD	59–115	0.295	1.05
SCZ	157	84.08 ± 8.79 SD	61–111	<0.001	1.87	129.07 ± 9.61 SD	99–158	0.027	1.22
SCZ2	948	533.29 ± 21.59 SD	469–615	<0.001	1.78	736.55 ± 22.32 SD	676–813	< 0.001	1.29
SCZ2 (5×10^{-8})[b]	134	6.43 ± 2.52 SD	0–18	<0.001	20.94	13.37 ± 3.32 SD	4–24	< 0.001	10.02
ADHD	29	55.69 ± 7.14 SD	36-79	<0.001[c]	−1.89	42.23 ± 5.78 SD	25–63	0.012[c]	−1.44
ASD	34	63.73 ± 7.62 SD	44–91	<0.001[c]	−1.85	114.94 9.09 SD	80–147	< 0.001[c]	−3.35
MDD	282	210 ± 13.9 SD	168–255	<0.001	1.34	218.11 ± 13.49 SD	174–268	< 0.001	1.29
CD	149	83.16 ± 8.89 SD	61–112	<0.001	1.8	150.5 ± 10.27 SD	121–182	0.591	−1.006
RA	396	71.9 ± 8.06 SD	46–100	<0.001	5.56	372.37 ± 16.08 SD	323–430	0.078	1.06
Height	350	146.01 ± 11.9 SD	108–188	<0.001	2.4	340.84 ± 14.91 SD	294–390	0.268	1.03

Schizophrenia, SCZ; bipolar disorder, BPD; attention deficit-hyperactivity disorder, ADHD; Crohn's disease, CD; autism spectrum disorder, ASD; major depressive disorder, MDD; cross-disorder associations, CDA; rheumatoid arthritis, RA.
[a]Proportion of the number of GR-response eSNPs observed for 1,000 permuted random SNPs and baseline eSNPs.
[b]Overlap at genome-wide significance level.
[c]Negative enrichment and inverse fold enrichment.

that a subset of MDD-related GR genes is also regulated by acute social defeat, providing an important extension to stress-related risk for depression.

Cumulative Risk Scores for the MDD-Related GR eSNPs Correlate with Dysfunctional Amygdala Reactivity

To investigate the relationship between MDD-related GR eSNPs and variability in stress-related brain function in humans, we applied an imaging genetics strategy to data from 647 participants (171 individuals with current or past DSM-IV Axis I disorders and 476 controls; 306 of participants were self-reported European-Americans [EUR-AM]; Table S5 and see also Experimental Procedures) of the Duke Neurogenetics Study (DNS) (see Experimental Procedures). Our analyses focused on centromedial amygdala reactivity to canonical threat-related angry and fearful facial expressions (Figure 7A), because this phenotype is clearly implicated in the etiology and pathophysiology of stress-related disorders, including depression (Phillips et al., 2003). Moreover, amygdala reactivity can trigger rapid physiological and behavioral responses to threat, including activation of the stress hormone response via projections from the medial division of the central nucleus of the amygdala, (captured in our analysis by our centromedial amygdala region of interest) to the paraventricular nucleus of the hypothalamus (Ulrich-Lai and Herman, 2009). Lastly, amygdala function is influenced by the slow-acting, presumably genomic effects of hydrocortisone administration (Henckens et al., 2010), further highlighting its importance as a systems-level phenotype sensitive to our observed GR-induced transcriptional responses.

Higher MDD-related GR tag eSNP GRPSs (Table S4; see also Experimental Procedures) were associated with blunted centromedial amygdala response to angry and fearful facial expressions relative to neutral expressions in the EUR-AM subsample, even after accounting for age, sex, and the presence of an Axis I disorder ($F_{1,301} = 7.06$, p = 0.008; Figure 7B). This effect was also observed in the entire sample after accounting for population stratification ($F_{1,637} = 6.05$, p = 0.014; Figure S4A). Permutation analyses that formed random SNP profiles (n = 1,000; matched for MAF and not exceeding the maximum correlation among profile SNPs; see Experimental Procedures) indicated that the actual GRPS were more likely to be associated with these differences in amygdala reactivity than 1,000 sets of random SNP profiles (EUR-AM subsample: permutation-based FDR = 0.003; entire sample: permutation-based FDR = 0.012). Post hoc analyses revealed that this differential effect was driven by higher centromedial amygdala reactivity to neutral facial expressions relative to our control condition in participants with higher GRPS (EUR-AM subsample: $F_{1,301} = 6.47$, p = 0.011; Figure 7D; entire sample: $F_{1,637} = 8.52$, p = 0.004; Figures S4A and S4C). There were no effects of GRPS on amygdala reactivity to angry and fearful facial expressions relative to our control condition (EUR-AM subsample: $F_{1,301} = 0.2$, p = 0.65; Figure 7C and entire sample: $F_{1,637} = 0.09$, p = 0.76; Figures S4A and S4B).

This pattern of altered amygdala reactivity in individuals with higher GRPS is suggestive of impaired threat-related cue learning with inappropriately increased reactivity to neutral expressions, which do not convey threat (Britton et al., 2011; Oliveira et al., 2013). Thus, higher GRPS may be associated with non-specific or overgeneralized threat and stress responses, which are consistently observed in depression as well as other mood and anxiety disorders (Britton et al., 2011; Oliveira et al., 2013).

DISCUSSION

We have shown that common variants in long-range enhancer elements alter the transcriptional responsiveness of GR target

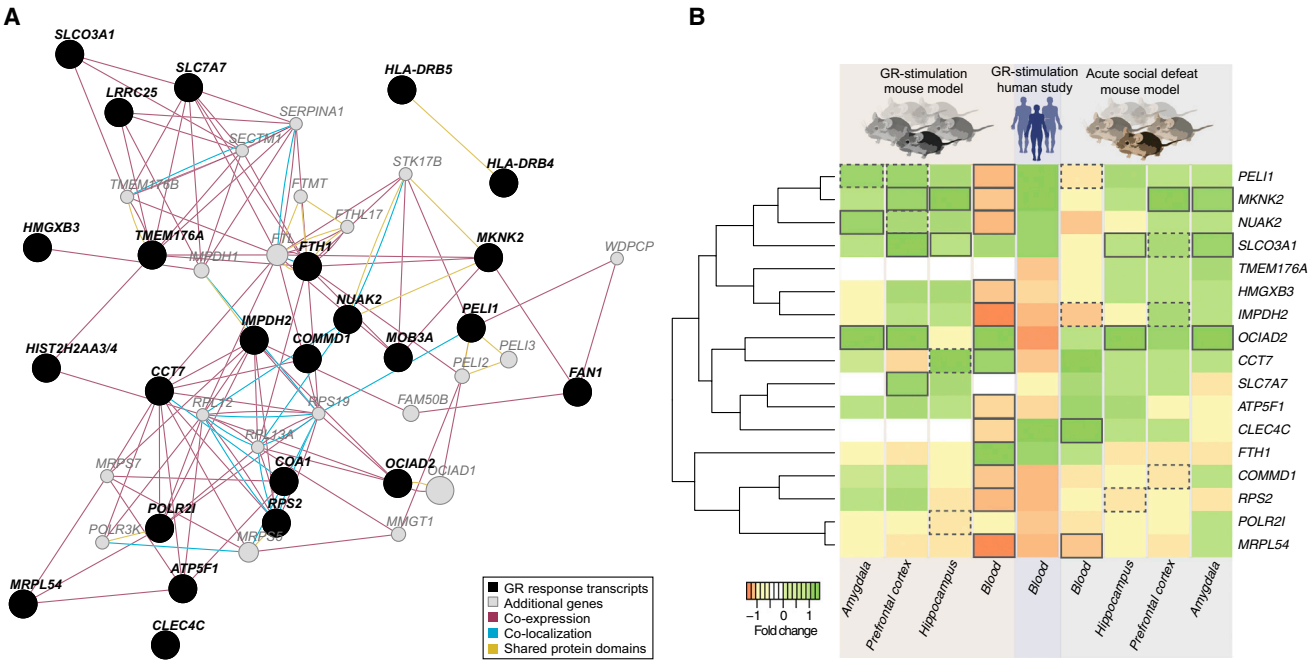

Figure 6. Functional Annotation of Transcripts Regulated by MDD-Related GR Risk Variants

(A) Gene network produced using GeneMANIA. The network consists of 43 genes (circles) connected by 164 interactions (edges). Genes that are within a black filled circle indicate our MDD-related GR transcripts (n = 24), while those within a gray filled circle indicate additional genes (n = 20). The interactions found between these genes, which were more enriched than expected, are shown (co-expression: purple lines, shared protein domains: yellow lines, and co-localization: blue lines).

(B) Heatmap of gene expression changes (log_2) between stress versus vehicle groups of mouse in brain and blood (n = 17 mice, left panel) as well as between baseline and GR-stimulation in human blood cells (blue, middle panel) and in mouse brain and blood (n = 22 mice, right panel). Investigated tissues are labeled within the bottom row of the heatmap (prefrontal cortex [PFC], hippocampus [HC], and amygdala [AM]). p values were computed by using linear regression model, and significance is indicated by a black box (FDR $\leq$ 0.1, dotted box p $\leq$ 0.05).

genes to the GR and that these variants cumulatively increase the risk for psychiatric disorders, including MDD and SCZ. These findings suggest that the risk of developing MDD after adverse life events may be influenced by an individual's sensitivity to the downstream, transcriptional effects of cortisol released during the stressful adverse events. In addition, the findings suggest that the changes seen in the initial transcriptional response to stress may influence how an individual processes stressful exposures. Indeed, the risk variants were also associated with overgeneralized centromedial amygdala reactivity to non-threat stimuli. This is consistent with dysfunctional behavioral and physiological hyper-responsiveness to threat in MDD and other psychiatric disorders.

One of our notable genetic findings is that the distance between the GR-response eSNPs and the regulated gene expression probe was significantly longer than the distances previously reported for baseline eQTLs (149 kb baseline eQTLs versus 406 kb for GR-response eQTLs in our dataset). Our data support and extend previous observations that indicated a long-range transcriptional regulation by the GR (Hakim et al., 2011; John et al., 2011; So et al., 2007). In fact, a combined analysis of our GR-response eQTLs and ChIA-PET data from the ENCODE project (ENCODE Project Consortium, 2011) as well as a validation using 3C analysis suggests that there could be a physical long-range interaction between the eSNP locus and the promoter of the GR-regulated transcript for at least 25% of the GR-response eQTLs. Additional experiments are necessary in order to investigate the direct effects of the different alleles on the enhancer function and chromatin conformation in other tissues, including the brain, to further validate this.

More broadly, our results indicate that stimulated eQTL approaches using disease-risk-relevant transcriptional stimuli (in our case GR activation and stress) can identify novel risk genes for common disorders that may otherwise go undetected. Previous studies have used eQTLs or DNA methylation QTLs (mQTLs) for the annotation of GWAS results and indicated the importance of using eQTLs and mQTLs from disease-relevant tissues (Gamazon et al., 2013; Nicolae et al., 2010). While we do not observe a significant enrichment of baseline blood eQTLs, GR-response eQTLs from this tissue were significantly enriched, even over baseline SNPs, among the variants associated with MDD and SCZ (see Table 1). Interestingly, GR-response eSNPs identified in whole blood were enriched in enhancers specific to brain tissue, while this was not the case for baseline eSNPs identified in blood (see Figures 3 and S2). This suggests that GR-response eSNPs may have more relevance for cross-tissue effects, especially in the brain. This pattern may underlie the observation that GR-response eSNPs were associated with psychiatric disorders and amygdala function, but not with other medical disorders or height. Our findings support the notion that not only the tissue

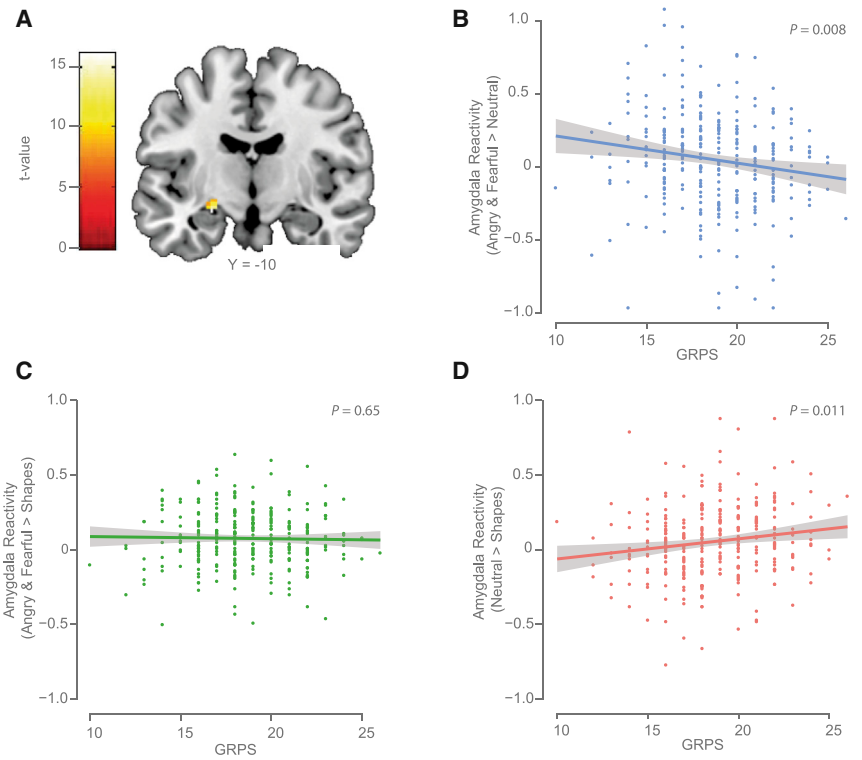

Figure 7. GR-Response MDD-Related eSNP GRPS Correlate with Overgeneralized Amygdala Reactivity

(A) Statistical parametric map illustrating left centromedial amygdala reactivity to facial expressions with an "Angry & Fearful > Neutral" contrast in the entire sample (15 contiguous voxels; max voxel MNI coordinate, x = −24, y = −10, z = −14, t = 4.35, p = 7.76 × 10^{-6}).

(B) Higher MDD-related GR eSNP genetic risk profile scores (GRPSs) in the European-American subsample of the DNS cohort (n = 306) predicted amygdala reactivity to threat-related facial expressions in comparison to neutral facial expressions.

(C and D) Post hoc analyses revealed that GRPSs did not predict amygdala reactivity to threat-related expressions (C), but that higher GRPSs predicted elevated amygdala reactivity to neutral facial expressions (D) in comparison to non-face control stimuli. The 95% confidence interval is displayed as gray shaded band in (B)–(D).

but also the type of stimulation, e.g., mimicking aspects of stress in our experiments, can be relevant for using such QTL studies in annotating GWAS results.

While these common genetic variants were discovered in peripheral blood cells, we provide evidence for their importance in neural circuits that are critical for generating and regulating the stress axis response to adversity. First, GR-response eSNP regions are enriched in enhancers relevant in brain tissue. Second, a number of the transcripts affected by these MDD-related GR eSNPs in their GR-regulated gene expression in human blood were also regulated by short-term GR activation or following exposure to acute social defeat stress in the mouse hippocampus, prefrontal cortex, or amygdala. Third, using imaging genetics, we demonstrate that the cumulative MDD-related GR tag eSNP genetic risk profile predicts overgeneralized reactivity of the human amygdala. It has to be noted, however, that while the GR-response eQTLs were identified using the selective GR agonist dexamethasone, the GR shares response elements with other steroid receptors, especially the mineralocorticoid receptor, so that we cannot exclude an important contribution of these other receptors.

Furthermore, the MDD-related GR genes formed a strongly interconnected gene network (over 85% of the genes are co-expressed; Figure 6A). Within this network, inflammation was the pathway with the highest connectivity (see Figure S3), and a number of studies indicate the pathophysiological relevance of this system in the development of MDD and SCZ (Haroon et al., 2012; Keller et al., 2013; Miller et al., 2009). The role of the immune system was also supported by results of the latest GWAS meta-analysis for SCZ (Schizophrenia Working Group of the Psychiatric Genomics Consortium, 2014). The connectivity of this system was followed in strength by the connectivity of proteasome degradation. It has been shown, for example, that activation of GRs enhances ubiquitin/proteasome-mediated degradation of glutamate receptor subunits and thereby mediates cognitive impairment induced by repeated stress exposure (Yuen et al., 2012). Genetic modulation of GR effects on the immune system in addition to ubiquitin/proteasome-mediated degradation thus provide a mechanistic link between risk for psychiatric disorders and the genetic differences in GR-induced gene expression.

Most importantly, our GR-response eQTL analysis revealed an enrichment of these GR-response eSNPs among MDD-associated SNPs over baseline eSNP sets as well as random SNP sets. This suggests that SNPs altering the initial transcriptional response to stress also influence the risk for MDD. The association was verified in an independent cohort. Furthermore, the increased risk conferred by these functional variants may extend to SCZ. This is consistent with evidence from recent studies of psychiatric disorders, which suggest shared genetic risk loci, with MDD having the highest co-heritability with BPD followed by SCZ (Lee et al., 2013). The fact that we do not detect a significant enrichment of GR-response eSNPs with BPD, despite the large SNP co-heritability of this disorder with both SCZ and MDD, may in part be due to the smaller sample size in this meta-analysis and thus insufficient power to detect true associations (n = 6,704 cases for BPD versus over 9,000 cases for MDD and SCZ1). The fact that the fold enrichment of GR-response eSNPs with SCZ increases with sample size (SCZ1: n = 9,087 cases versus SCZ2: n = 36,989 cases) and p value cut-off ($p < 0.05$ and $p < 5 \times 10^{-8}$) suggests that the strategy of using stimulated eQTL approaches may help in identifying true associations for disease. Interestingly, we find that four MDD-related GR eQTL bins, which are not only associated with MDD but

also with SCZ, and the cross-disorder associations from the PGC analyses (Table 1) reach genome-wide significance for SCZ in the most recent meta-analysis (Schizophrenia Working Group of the Psychiatric Genomics Consortium, 2014). Besides the extended MHC region (chr6: 26–34 Mb, hg19), these overlapping risk loci include a region on chr1: 149,998,890–150,242,490 (hg19) that now ranks 48th for association with SCZ and overlaps with the MDD-related GR eQTL bin, *ANP32/PLEKHO1*, that regulates the probe gene *HIST2H2AA3/4.* This GR-response eQTL drives the overlap with genome-wide SCZ2 associations, and it has been validated using qPCR (Supplemental Information). These findings suggest that GR-response eSNPs may contribute to the shared risk between psychiatric disorders, especially MDD and SCZ, and that this approach may delineate between shared and specific risk factors for these disorders.

Results from our imaging genetics study provide one potential neural pathway by which MDD-related GR eSNPs may increase the risk for the development of stress-related psychopathology, including depression. Interestingly, MDD-related GR eSNPs predict heightened amygdala reactivity to stimuli that do not inherently signal threat (i.e., neutral facial expressions). This suggests that MDD-related GR eSNPs associated with the immediate transcriptome response to stress may impair the neural circuitry that supports the learning of threat-related cues and, possibly, thereby contribute to the overgeneralization of threat-related stress responses. Indeed, in healthy individuals, the genomic effects of hydrocortisone result in more specific reactivity to threatening stimuli (Henckens et al., 2010). As such, MDD-related GR eSNPs may underpin a less adaptive and overgeneralized amygdala response that leaves individuals more likely to perceive threat in the absence of unambiguous cues; this in turn may lead to the development of cognitive biases associated with depression, or perhaps even paranoia, in the context of schizophrenia.

The data presented in this study show that common genetic variants that change the GR-mediated immediate transcriptome response to stress are linked, in the long-term, to both changes in neural processing of threat and increased risk for MDD and SCZ. Our data lend further support to the notion of a possible shared genetic liability of some psychiatric disorders and specifically point to stress-responsive genes as common risk factors. Studies dissecting how these genetic variants alter the molecular, cellular, and neural response to glucocorticoids in the short and long term could inform the development of novel strategies for the prevention and treatment of stress-related psychiatric disorders.

EXPERIMENTAL PROCEDURES

Samples and Study Designs

MPIP Cohort

The subject pool for the eQTL analysis consisted of 164 male Caucasian individuals: 93 healthy probands and 71 in-patients with depressive disorders treated at the Max Planck Institute of Psychiatry's hospital in Munich, Germany (MPIP cohort; see Supplemental Experimental Procedures; Hennings et al., 2009; Menke et al., 2012 for details). Baseline whole-blood samples (for plasma and RNA) were obtained at 6 p.m. after 2 hr of fasting and abstention from coffee and physical activity. Immediately afterward the participants were given 1.5 mg dexamethasone orally. A second blood draw was performed 3 hr later at 9 p.m. (see Figure 2A). Cortisol and ACTH serum levels were determined using previously described radioimmunoassays (Hennings et al., 2009; Menke et al., 2012). Plasma dexamethasone concentrations were assessed in serum samples drawn at 9 p.m. using liquid chromatography-tandem mass spectrometry on API4000 (AB Sciex).

MARS Cohort

This sample included 1,483 participants with European ancestry (1,005 with MDD) recruited for the MARS project at the MPIP in Munich. All individuals used within the eQTL study (MPIP cohort) were not part of this sample (see Supplemental Experimental Procedures and Hennings et al., 2009 for details).

DNS Cohort

The imaging genetics analysis was conducted on data from (1) a European-American subsample of 306 participants (63 with DSM-IV Axis I disorder) and (2) a full sample of 647 participants (117 with DSM-IV Axis I disorder) of the ongoing Duke Neurogenetics Study (see Supplemental Experimental Procedures). All participants completed a widely utilized functional magnetic resonance imaging (fMRI) paradigm assessing threat-related amygdala reactivity (see Supplemental Experimental Procedures).

Mouse Models

Twenty-two male C57BL/6N mice were used for the dexamethasone-stimulation test (DEX-mouse). The experiment was performed twice with two separate batches of mice (n = 22 per batch). Animals were injected i.p. with either vehicle (VEH, n = 11) or 10 mg/kg dexamethasone (DEX, n = 11) between 9 a.m. and 11 a.m. Animals were sacrificed 4 hr post-injection.

The acute social defeat sample included 17 male C57BL/6N mice (n = 8 control and n = 9 acute stress mice) taken from a larger study that were used for this experiment. Mice underwent the acute social defeat stress once exactly 4 hr preceding sacrifice and tissue collection. The acute social defeat paradigm was performed as described previously (Wagner et al., 2013) on a single day between 9 a.m. and 12 p.m. (see Supplemental Experimental Procedures).

From both animal models described above, blood was collected and the brain was carefully extracted and dissected (see Supplemental Experimental Procedures). The following brain regions were collected: hippocampus (HC), prefrontal cortex (PFC), and the amygdala (AM).

All human studies have been approved by the respective local ethics committees and all individuals gave written informed consent. Details about the individual studies are listed below or in the Supplemental Experimental Procedures. The mouse model protocols were approved by the Committee for the Care and Use of Laboratory Animals of the Government of Upper Bavaria, Germany.

Gene Expression Data

The human whole-blood RNA of the MPIP cohort samples was hybridized to Illumina HumanHT-12 v3.0 array. All array probes have been subjected to an extensive quality control (QC; see Supplemental Experimental Procedures). For the GR-response eQTL analysis, only transcripts that showed a difference in gene expression between the samplings at 6 p.m. and 9 p.m. with an absolute fold change $\geq$ 1.3 in at least 20% of all samples were categorized as robustly effected by dexamethasone stimulation (n = 4,630 transcripts) and further used in the analysis. The position of the array probes and possible SNPs within these sequences were annotated using ReMOAT version August 2009 (Barbosa-Morais et al., 2010), leaving 4,447 autosomal array probes for the GR-response eQTL analysis (see Supplemental Experimental Procedures).

DEX-mouse RNA samples were hybridized on Illumina MouseRef-8 v2.0 chips, and the mouse RNA from the acute social defeat mouse model was hybridized on Illumina MouseWG-8 v2.0 chips. QC was applied separately for each tissue and experiment as described in Supplemental Experimental Procedures.

Genotype Data

Human DNA from MPIP and MARS cohort subjects was extracted from EDTA blood samples and genotyped on Illumina Human610-Quad/Human660W-Quad arrays (MPIP cohort) and Illumina Sentix Human-1/HumanHap300/Human610-Quad/HumanOmniExpress arrays (MARS cohort). From the SNP

data surviving QC, imputation of additional variants was performed using IMPUTE v2 (Howie et al., 2009; see Supplemental Experimental Procedures for more detail on genotyping QC and imputation).

The MARS GRPSs included alleles from 20 of the 23 tag eSNPs (three SNPs diverged from HWE in the MARS sample, see Table S3). See also Supplemental Experimental Procedures.

Human DNA from participants of the DNS cohort was isolated from saliva and genotyped on the Illumina HumanOmniExpress array as well as a custom array containing an additional ~300,000 SNPs. The DNS GRPSs included alleles from 19 of the 23 tag eSNPs (four SNPs not present on genotyping array; see Table S4 and Supplemental Experimental Procedures).

Statistical Analysis

The eQTL analysis (MPIP cohort) was restricted to those SNP-probe pairs that map within a region of 1 Mb upstream or downstream of the gene expression probe, in order to detect *cis*-eQTLs. To measure the transcriptional response, we used the log fold change in gene expression changes between 6 p.m. (baseline) and 9 p.m. (GR-stimulation) standardized to baseline.

PLINK v1.07 (Purcell et al., 2007) was used to test for *cis*-association between all imputed SNPs and transcriptional response. As eQTL data were composed of two kinds of data, genotyping and expression data, we used two stages of multiple testing correction: (1) SNP level correction: for each *cis*-region (array probe), we performed a permutation test. The sample identifiers in the gene expression data were shuffled in order to preserve the structure in the genotype data (LD). A total of 500,000 permutations were carried out per probe, and the empirical p values were adjusted using the Westfall-Young correction for the number of SNPs per probe, i.e., maxT procedure of Westfall-Young (Westfall and Young, 1993). (2) Probe level correction: *cis*-regions with an extensive LD structure will increase the number of false positive eQTLs (Westra et al., 2013). Therefore, we applied the Benjamini-Hochberg method to correct the maxT-adjusted p value significance by using only the most significant and independent SNPs per probe (tag SNPs). The number of tag eSNPs per *cis*-region was identified by LD pruning and "clumping" the SNPs using the "clump" command in PLINK (using distance < 1 Mb and $r^2 \leq 0.2$ as setting). Each tag SNP forms a SNP bin by aggregating SNPs at $r^2 \leq 0.2$ and distance < 1 Mb. SNPs within a given bin were correlated to the tag SNP, but not to any other tag SNP of an other SNP bin. We limited the false-positive SNP-probe pairs to less than 5% and therefore considered the FDR analog of the p value (Q value) < 5% as statistically significant.

Validation of GR-response *cis*-eQTL results was carried out with a sample size-weighted *Z* score meta-analysis (Evangelou and Ioannidis, 2013) in an additional independent dataset using peripheral blood samples of 58 individuals (see Supplemental Experimental Procedures). A GR-response *cis*-eQTL was validated if the meta-analysis p value was less than the actual maxT-adjusted p value in the discovery sample alone.

The genomic control inflation factor (λ_{gc}; Devlin and Roeder, 1999) was calculated for every GR-response eQTL gene expression probe (n = 297) based on the genome-wide genotype data (λ_{gc}). The inflation factor was computed in PLINK as median χ^2 statistic. The median λ_{gc} over all probes is 1, which implies no large inflation was present.

We used *NR3C1* ChIP-seq data obtained from the ENCODE Project (ENCODE Project Consortium, 2011) to determine actual GR binding at GR-response eSNPs (see Supplemental Experimental Procedures).

To determine whether GR-response eSNPs were enriched for functional regions, we annotated them using HaploReg (Ward and Kellis, 2012) and compared the results to a realistic null distribution based on permuted baseline eSNP sets (see Supplemental Experimental Procedures).

ChIA-PET data were obtained from the UCSC Genome Browser (http://hgdownload.cse.ucsc.edu/goldenPath/hg19/encodeDCC/wgEncodeGisChiaPet; see Supplemental Experimental Procedures).

To identify whether GR-response eSNPs were enriched for association with MDD, SCZ, BPD, ADHD, ASD, Crohn's disease, rheumatoid arthritis, and the GWAS loci for height, we integrated our data with results from the previously published GWAS analysis (see Supplemental Experimental Procedures). To prove the significance of the MDD-related GR SNPs for MDD, we used a logistic regression model to test the association of the MDD-related GR tag eSNP GRPSs for disease status in the independent MARS cohort. Gender, BMI, and age were used as covariates. To establish the null distribution, we generated 1,000 random SNP profiles by swapping individual labels to provide new SNP profiles under the null hypothesis. To further account for the genomic LD structure, we limited the analyses to tag SNPs (tag SNP = SNP showing the highest association per *cis*-eQTL bin) and generated 1,000 randomized SNP sets; conditional on MAF and each of the same size as the GR-response tag SNPs overlap with MDD associations (n = 285).

The gene network analysis was performed using the online tool GeneMANIA (Montojo et al., 2014). To establish the null-distribution, we calculated the gene network for ten sets of randomly chosen GR-response transcripts (n = 4,422). Finally, we determined the average gene network results in order to establish the relationship between MDD-relevant GR-response transcripts and non-MDD-relevant but GR-response transcripts. Network categories showing a fold enrichment > 1 are reported in Figure 6A.

For the co-expression analysis, we used the GR-response residuals from all array probes (n = 4,422) to determine if the 25 MDD-related GR array probes are more co-regulated than 1,000 sets of randomly chosen GR-stimulated transcripts (see Supplemental Experimental Procedures).

A disease-related network was built by manual curation and literature mining using the CIDeR database (Lechner et al., 2012) and the yED software (yWorks GmbH, Tübingen).

To test the relationship of the GR-response eSNPs and threat-related amygdala reactivity, we used an imaging genetics strategy as described in the Supplemental Experimental Procedures.

Chromatin Conformation Capture Analysis

3C was carried out in five LCLs as described in Hagège et al., 2007 and detailed in the Supplemental Experimental Procedures.

qPCR Validation

Quantitative real-time PCR (qPCR) was used to validate the association between eSNPs and GR-stimulated gene expression of *ADORA3* (the probe with the most significant GR-response eQTL) and *HIST2H2AA3*/*HIST2H2AA4* (the probe with the most eSNPs overlapping with data from our meta-analysis for MDD) in whole blood cells and for a long-range GR-response eQTL-*NRTN* in five LCLs, which were also used with the 3C assay. More details are provided in Supplemental Experimental Procedures.

ACCESSION NUMBERS

Data from the human gene expression microarray experiment were deposited at the GEO repository under GEO: GSE46743.

SUPPLEMENTAL INFORMATION

Supplemental Information includes Supplemental Experimental Procedures, four figures, six tables, and the list of collaborators of the Major Depressive Disorder Working Group of the Psychiatric Genomics Consortium and can be found with this article online at http://dx.doi.org/10.1016/j.neuron.2015.05.034.

ACKNOWLEDGMENTS

This study has received its main financial support from the European Union under European Research Council GA no. 281338 (to E.B.B.) and was also supported by the BMBF within the Program for Medical Genome Research with the Research Grant FKZ 01GS08151 (to W.W.) and financed by the DFG within the Cooperation Clinical Group Molecular Neurogenetics (WU 164/3-2) and the Helmholtz Alliances of Systems Biology and of Mental Health in an Ageing Society Grant HA-215 (W.W.). J.A. was supported in part by the NeuroNova gGmbH, A.R.H. by NIH (NIDA R01-DA031579), R.B. by the Klingenstein Third Generation Foundation and McDonnell Center for Systems Neuroscience, and C.E.C. by an NSF pre-doctoral grant (DGE-1143954). The Duke Neurogenetics Study (DNS) is supported by Duke University and the NIH (NIDA R01-DA033369). We thank D. Spengler, A. Hoffmann, M. Rex-Haffner, S. Darchinger, A. Löschner, and M. Ködel for excellent technical support. We are

grateful to S. Röh for processing the NR3C1 ChIP-seq data. We also thank L. Preis and A. Eichelkraut for recruitment and sample ascertainment of the Max-Planck Institute of Psychiatry (MPIP) cohort and Y.S. Nikolova, A.X. Gorka, B. Brigidi, K. Faig, S. Jacobson, and A. Knodt for assistance with DNS cohort data collection.

See Supplemental Information for the full list of collaborators of the Major Depressive Disorder Working Group of the Psychiatric Genomics Consortium (PGC).

Received: October 20, 2014
Revised: March 26, 2015
Accepted: May 13, 2015
Published: June 3, 2015

REFERENCES

Barbosa-Morais, N.L., Dunning, M.J., Samarajiwa, S.A., Darot, J.F.J., Ritchie, M.E., Lynch, A.G., and Tavaré, S. (2010). A re-annotation pipeline for Illumina BeadArrays: improving the interpretation of gene expression data. Nucleic Acids Res. *38*, e17.

Britton, J.C., Lissek, S., Grillon, C., Norcross, M.A., and Pine, D.S. (2011). Development of anxiety: the role of threat appraisal and fear learning. Depress. Anxiety *28*, 5–17.

de Kloet, E.R., Joëls, M., and Holsboer, F. (2005). Stress and the brain: from adaptation to disease. Nat. Rev. Neurosci. *6*, 463–475.

Devlin, B., and Roeder, K. (1999). Genomic control for association studies. Biometrics *55*, 997–1004.

Dohrenwend, B.P., and Egri, G. (1981). Recent stressful life events and episodes of schizophrenia. Schizophr. Bull. *7*, 12–23.

ENCODE Project Consortium (2011). A user's guide to the encyclopedia of DNA elements (ENCODE). PLoS Biol. *9*, e1001046.

Evangelou, E., and Ioannidis, J.P.A. (2013). Meta-analysis methods for genome-wide association studies and beyond. Nat. Rev. Genet. *14*, 379–389.

Gamazon, E.R., Badner, J.A., Cheng, L., Zhang, C., Zhang, D., Cox, N.J., Gershon, E.S., Kelsoe, J.R., Greenwood, T.A., Nievergelt, C.M., et al. (2013). Enrichment of cis-regulatory gene expression SNPs and methylation quantitative trait loci among bipolar disorder susceptibility variants. Mol. Psychiatry *18*, 340–346.

Hagège, H., Klous, P., Braem, C., Splinter, E., Dekker, J., Cathala, G., de Laat, W., and Forné, T. (2007). Quantitative analysis of chromosome conformation capture assays (3C-qPCR). Nat. Protoc. *2*, 1722–1733.

Hakim, O., Sung, M.-H., Voss, T.C., Splinter, E., John, S., Sabo, P.J., Thurman, R.E., Stamatoyannopoulos, J.A., de Laat, W., and Hager, G.L. (2011). Diverse gene reprogramming events occur in the same spatial clusters of distal regulatory elements. Genome Res. *21*, 697–706.

Haroon, E., Raison, C.L., and Miller, A.H. (2012). Psychoneuroimmunology meets neuropsychopharmacology: translational implications of the impact of inflammation on behavior. Neuropsychopharmacology *37*, 137–162.

Heim, C., and Binder, E.B. (2012). Current research trends in early life stress and depression: review of human studies on sensitive periods, gene-environment interactions, and epigenetics. Exp. Neurol. *233*, 102–111.

Henckens, M.J.A.G., van Wingen, G.A., Joëls, M., and Fernández, G. (2010). Time-dependent effects of corticosteroids on human amygdala processing. J. Neurosci. *30*, 12725–12732.

Hennings, J.M., Owashi, T., Binder, E.B., Horstmann, S., Menke, A., Kloiber, S., Dose, T., Wollweber, B., Spieler, D., Messer, T., et al. (2009). Clinical characteristics and treatment outcome in a representative sample of depressed inpatients - findings from the Munich Antidepressant Response Signature (MARS) project. J. Psychiatr. Res. *43*, 215–229.

Howie, B.N., Donnelly, P., and Marchini, J. (2009). A flexible and accurate genotype imputation method for the next generation of genome-wide association studies. PLoS Genet. *5*, e1000529.

Jankord, R., and Herman, J.P. (2008). Limbic regulation of hypothalamo-pituitary-adrenocortical function during acute and chronic stress. Ann. N Y Acad. Sci. *1148*, 64–73.

John, S., Sabo, P.J., Thurman, R.E., Sung, M.-H., Biddie, S.C., Johnson, T.A., Hager, G.L., and Stamatoyannopoulos, J.A. (2011). Chromatin accessibility pre-determines glucocorticoid receptor binding patterns. Nat. Genet. *43*, 264–268.

Keller, W.R., Kum, L.M., Wehring, H.J., Koola, M.M., Buchanan, R.W., and Kelly, D.L. (2013). A review of anti-inflammatory agents for symptoms of schizophrenia. J. Psychopharmacol. (Oxford) *27*, 337–342.

Kendler, K.S. (2013). What psychiatric genetics has taught us about the nature of psychiatric illness and what is left to learn. Mol. Psychiatry *18*, 1058–1066.

Kendler, K.S., and Karkowski-Shuman, L. (1997). Stressful life events and genetic liability to major depression: genetic control of exposure to the environment? Psychol. Med. *27*, 539–547.

Kendler, K.S., Gatz, M., Gardner, C.O., and Pedersen, N.L. (2006). A Swedish national twin study of lifetime major depression. Am. J. Psychiatry *163*, 109–114.

Kessler, R.C., Berglund, P., Demler, O., Jin, R., Merikangas, K.R., and Walters, E.E. (2005). Lifetime prevalence and age-of-onset distributions of DSM-IV disorders in the National Comorbidity Survey Replication. Arch. Gen. Psychiatry *62*, 593–602.

Kundaje, A., Meuleman, W., Ernst, J., Bilenky, M., Yen, A., Heravi-Moussavi, A., Kheradpour, P., Zhang, Z., Wang, J., Ziller, M.J., et al.; Roadmap Epigenomics Consortium (2015). Integrative analysis of 111 reference human epigenomes. Nature *518*, 317–330.

Lechner, M., Höhn, V., Brauner, B., Dunger, I., Fobo, G., Frishman, G., Montrone, C., Kastenmüller, G., Waegele, B., and Ruepp, A. (2012). CIDeR: multifactorial interaction networks in human diseases. Genome Biol. *13*, R62.

Lee, S.H., Ripke, S., Neale, B.M., Faraone, S.V., Purcell, S.M., Perlis, R.H., Mowry, B.J., Thapar, A., Goddard, M.E., Witte, J.S., et al.; Cross-Disorder Group of the Psychiatric Genomics Consortium; International Inflammatory Bowel Disease Genetics Consortium (IIBDGC) (2013). Genetic relationship between five psychiatric disorders estimated from genome-wide SNPs. Nat. Genet. *45*, 984–994.

McKay, L.I., and Cidlowski, J.A. (1999). Molecular control of immune/inflammatory responses: interactions between nuclear factor-kappa B and steroid receptor-signaling pathways. Endocr. Rev. *20*, 435–459.

Menke, A., Arloth, J., Pütz, B., Weber, P., Klengel, T., Mehta, D., Gonik, M., Rex-Haffner, M., Rubel, J., Uhr, M., et al. (2012). Dexamethasone stimulated gene expression in peripheral blood is a sensitive marker for glucocorticoid receptor resistance in depressed patients. Neuropsychopharmacology *37*, 1455–1464.

Miller, A.H., Maletic, V., and Raison, C.L. (2009). Inflammation and its discontents: the role of cytokines in the pathophysiology of major depression. Biol. Psychiatry *65*, 732–741.

Montojo, J., Zuberi, K., Rodriguez, H., Bader, G.D., and Morris, Q. (2014). GeneMANIA: Fast gene network construction and function prediction for Cytoscape. F1000Res. *3*, 153.

Nicolae, D.L., Gamazon, E., Zhang, W., Duan, S., Dolan, M.E., and Cox, N.J. (2010). Trait-associated SNPs are more likely to be eQTLs: annotation to enhance discovery from GWAS. PLoS Genet. *6*, e1000888.

Oliveira, L., Ladouceur, C.D., Phillips, M.L., Brammer, M., and Mourao-Miranda, J. (2013). What does brain response to neutral faces tell us about major depression? evidence from machine learning and fMRI. PLoS ONE *8*, e60121.

Phillips, M.L., Drevets, W.C., Rauch, S.L., and Lane, R. (2003). Neurobiology of emotion perception II: Implications for major psychiatric disorders. Biol. Psychiatry *54*, 515–528.

Phuc Le, P., Friedman, J.R., Schug, J., Brestelli, J.E., Parker, J.B., Bochkis, I.M., and Kaestner, K.H. (2005). Glucocorticoid receptor-dependent gene regulatory networks. PLoS Genet. *1*, e16.

Purcell, S., Neale, B., Todd-Brown, K., Thomas, L., Ferreira, M.A.R., Bender, D., Maller, J., Sklar, P., de Bakker, P.I.W., Daly, M.J., and Sham, P.C. (2007). PLINK: a tool set for whole-genome association and population-based linkage analyses. Am. J. Hum. Genet. *81*, 559–575.

Ripke, S., Wray, N.R., Lewis, C.M., Hamilton, S.P., Weissman, M.M., Breen, G., Byrne, E.M., Blackwood, D.H., Boomsma, D.I., Cichon, S., et al.; Major Depressive Disorder Working Group of the Psychiatric GWAS Consortium (2013). A mega-analysis of genome-wide association studies for major depressive disorder. Mol. Psychiatry *18*, 497–511.

Roussos, P., Mitchell, A.C., Voloudakis, G., Fullard, J.F., Pothula, V.M., Tsang, J., Stahl, E.A., Georgakopoulos, A., Ruderfer, D.M., Charney, A., et al. (2014). A role for noncoding variation in schizophrenia. Cell Rep. *9*, 1417–1429.

Schizophrenia Working Group of the Psychiatric Genomics Consortium (2014). Biological insights from 108 schizophrenia-associated genetic loci. Nature *511*, 421–427.

So, A.Y., Chaivorapol, C., Bolton, E.C., Li, H., and Yamamoto, K.R. (2007). Determinants of cell- and gene-specific transcriptional regulation by the glucocorticoid receptor. PLoS Genet. *3*, e94.

Tai, H.-C., and Schuman, E.M. (2008). Ubiquitin, the proteasome and protein degradation in neuronal function and dysfunction. Nat. Rev. Neurosci. *9*, 826–838.

Ulrich-Lai, Y.M., and Herman, J.P. (2009). Neural regulation of endocrine and autonomic stress responses. Nat. Rev. Neurosci. *10*, 397–409.

Ustün, T.B., Ayuso-Mateos, J.L., Chatterji, S., Mathers, C., and Murray, C.J.L. (2004). Global burden of depressive disorders in the year 2000. Br. J. Psychiatry *184*, 386–392.

van Rossum, E.F., Binder, E.B., Majer, M., Koper, J.W., Ising, M., Modell, S., Salyakina, D., Lamberts, S.W., and Holsboer, F. (2006). Polymorphisms of the glucocorticoid receptor gene and major depression. Biol. Psychiatry *59*, 681–688.

Wagner, K.V., Hartmann, J., Mangold, K., Wang, X.-D., Labermaier, C., Liebl, C., Wolf, M., Gassen, N.C., Holsboer, F., Rein, T., et al. (2013). Homer1 mediates acute stress-induced cognitive deficits in the dorsal hippocampus. J. Neurosci. *33*, 3857–3864.

Ward, L.D., and Kellis, M. (2012). HaploReg: a resource for exploring chromatin states, conservation, and regulatory motif alterations within sets of genetically linked variants. Nucleic Acids Res. *40*, D930–D934.

Warden, D., Rush, A.J., Trivedi, M.H., Fava, M., and Wisniewski, S.R. (2007). The STAR*D Project results: a comprehensive review of findings. Curr. Psychiatry Rep. *9*, 449–459.

Westfall, P.H., and Young, S.S. (1993). On Adjusting P-Values for Multiplicity. Biometrics *49*, 941–944.

Westra, H.-J., Peters, M.J., Esko, T., Yaghootkar, H., Schurmann, C., Kettunen, J., Christiansen, M.W., Fairfax, B.P., Schramm, K., Powell, J.E., et al. (2013). Systematic identification of trans eQTLs as putative drivers of known disease associations. Nat. Genet. *45*, 1238–1243.

Wilkinson, P.O., and Goodyer, I.M. (2011). Childhood adversity and allostatic overload of the hypothalamic-pituitary-adrenal axis: a vulnerability model for depressive disorders. Dev. Psychopathol. *23*, 1017–1037.

Yuen, E.Y., Wei, J., Liu, W., Zhong, P., Li, X., and Yan, Z. (2012). Repeated stress causes cognitive impairment by suppressing glutamate receptor expression and function in prefrontal cortex. Neuron *73*, 962–977.

Neuron, Volume *86*

Supplemental Information

Genetic Differences in the Immediate Transcriptome Response to Stress Predict Risk-Related Brain Function and Psychiatric Disorders

Janine Arloth, Ryan Bogdan, Peter Weber, Goar Frishman, Andreas Menke, Klaus V. Wagner, Georgia Balsevich, Mathias V. Schmidt, Nazanin Karbalai, Darina Czamara, Andre Altmann, Dietrich Trümbach, Wolfgang Wurst, Divya Mehta, Manfred Uhr, Torsten Klengel, Angelika Erhardt, Caitlin E. Carey, Emily Drabant Conley, Major Depressive Disorder Working Group of the Psychiatric Genomics Consortium (PGC), Andreas Ruepp, Bertram Müller-Myhsok, Ahmad R. Hariri, and Elisabeth B. Binder

SUPPLEMENTAL DATA

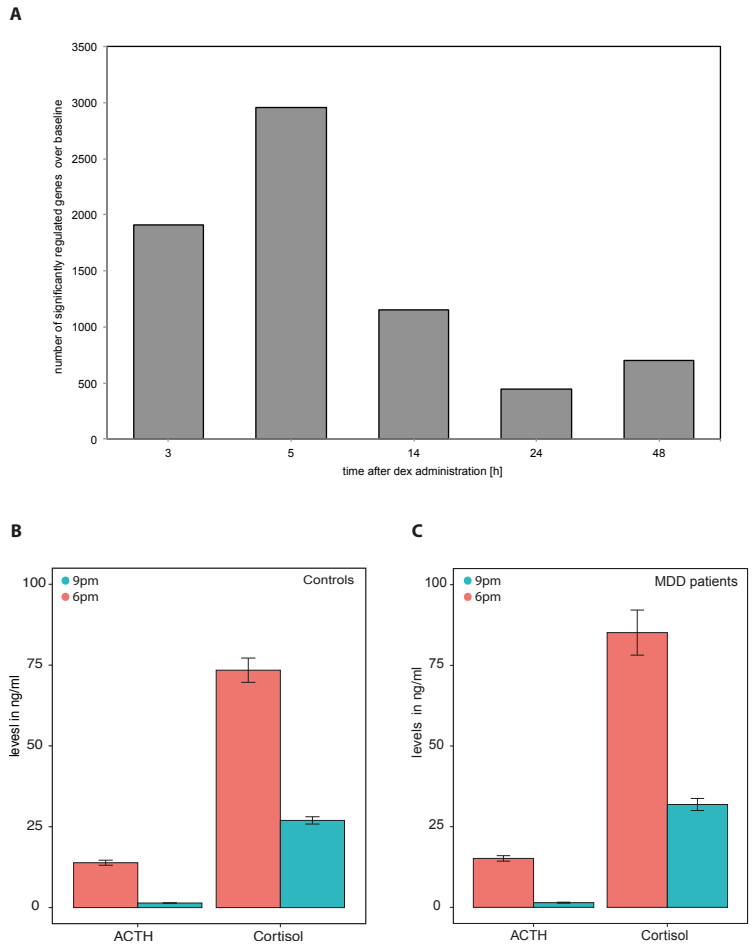

Figure S1. Related to Figure 2.

(A) Time course of gene expression changes after oral dexamethasone administration. The number of genes that are differently expressed at several time points after administration of 1.5 mg dexamethasone relative to baseline in 4 healthy male individuals are shown. The height of the bars indicates the total number of transcripts with nominally significant changes from baseline gene expression. Baseline blood samples were obtained at 6pm. This evening time point was chosen so that the stimulation experiments took place during the quiescent period of the stress hormone system. Baseline blood draws were immediately followed by oral administration of dexamethasone. Additional blood samples were drawn at 9pm and 11pm on the same day, at 8am and 6pm the next day and at 6pm on day 3. A comparison of baseline gene expression vs. gene expression after 3, 5, 14, 24 and 48 h shows an initial high number of gene expression changes, followed by a normalization within 24-48 hours. The highest number of differently expressed genes (highest bar in chart) was observed at 3 and 5 hours post dexamethasone ingestion. For practical reasons as well as to avoid secondary GR target effects, in the subsequent experiment we collected blood 3 hours after dexamethasone intake. (B), (C) Dexamethasone effect on cortisol and ACTH levels. Administration of dexamethasone resulted in a robust suppression of cortisol in all individuals. Cortisol levels were significantly suppressed in healthy controls (B; $F_{1,90} = 89.74$, $P = 3.57 \times 10^{-15}$) as well as in depressed patients (C; $F_{1,67} = 7.09$, $P = 0.0097$) 3h after dexamethasone challenge. Similar results were observed for ACTH, with a significant reduction in ACTH levels in healthy controls B; $F_{1,91} = 43.96$, $P = 2.33 \times 10^{-9}$) and in depressed patients (C; $F_{1,65} = 9.75$, $P = 0.0027$) after 3h.

P values in (A,B) derived from a linear model; error bars: ± sem

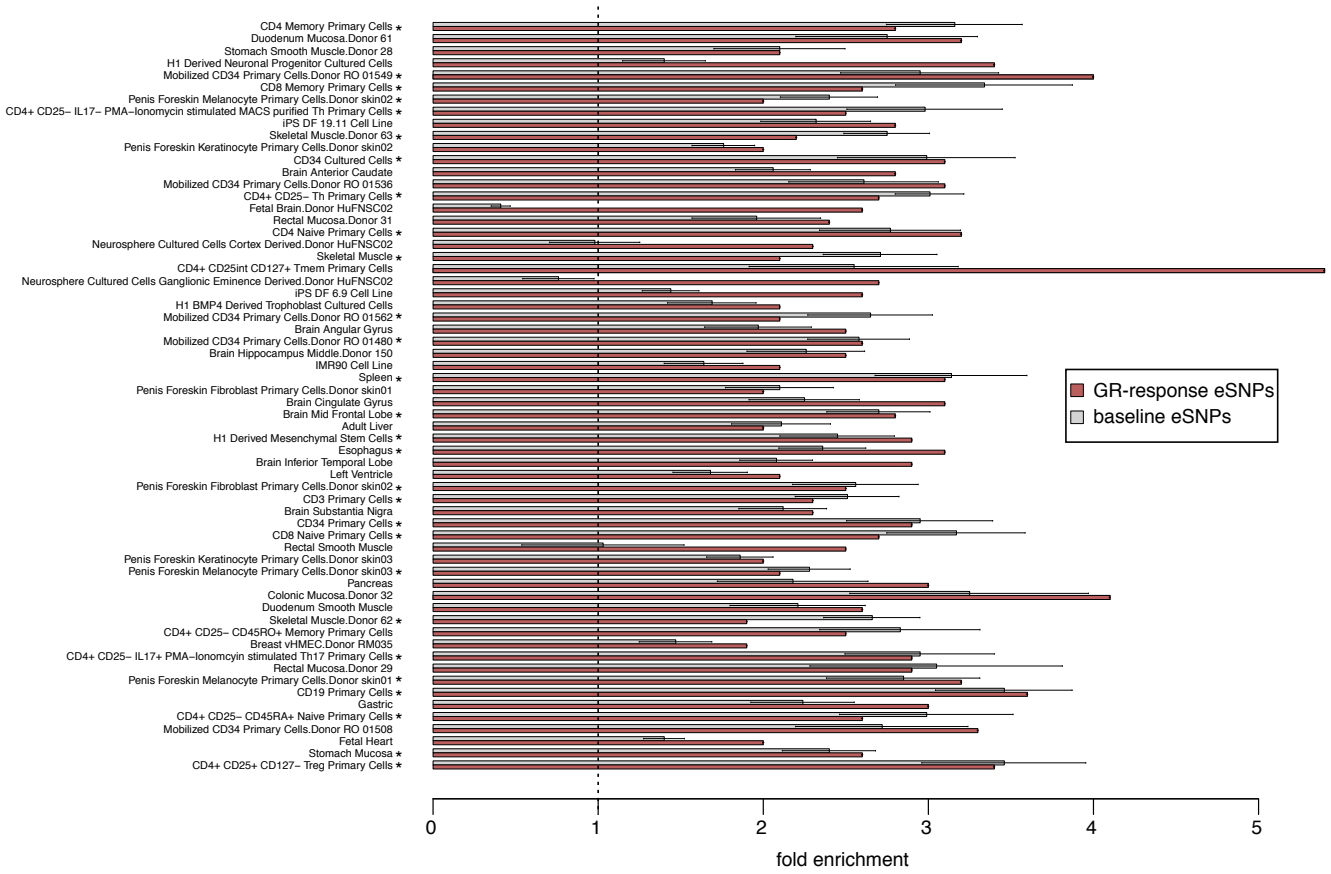

Figure S2. Related to Figure 3.

GR- eSNPs are enriched for enhancers in multiple tissues and cell lines from the Roadmap Epigenome Project. The x-axis shows the fold enrichment and the y-axis shows all enhancers that survived the Bonferroni multiple testing correction for the number of tested tissues or cells. GR-response eSNPs are illustrated in red and baseline eSNPs in gray. Out of the 62 presented enhancers, 28 additionally showed a significant enrichment within baseline eSNPs (marked with *).
P values derived from a binomial enrichment test; error bars: ± sd

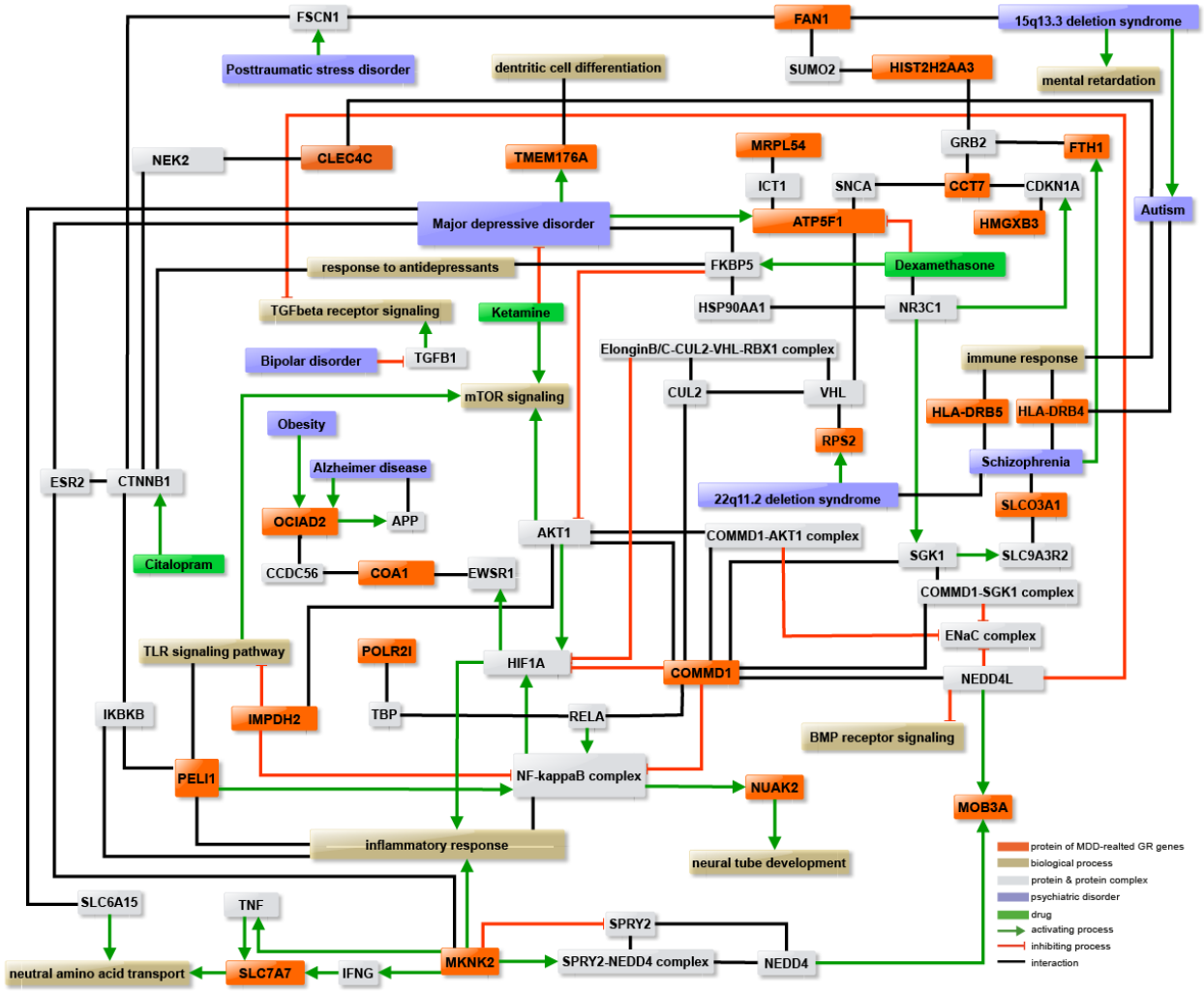

Figure S3. Related to Figure 6.
Disease-related network. For 22 of the 24 MDD-related GR genes a tightly interconnected disease-related network was generated from manually curated experimental data derived from the literature. Elements of the figure: Proteins from MDD-related GR genes (orange boxes), additional proteins and protein complexes (white boxes), biological processes (beige boxes), psychiatric disorders (blue boxes), drugs (green boxes), activating processes (green arrow-headed lines), inhibitory processes (red bar-headed lines) and interactions such as physical interactions, associations with diseases and differential regulation of signaling pathways (black line).

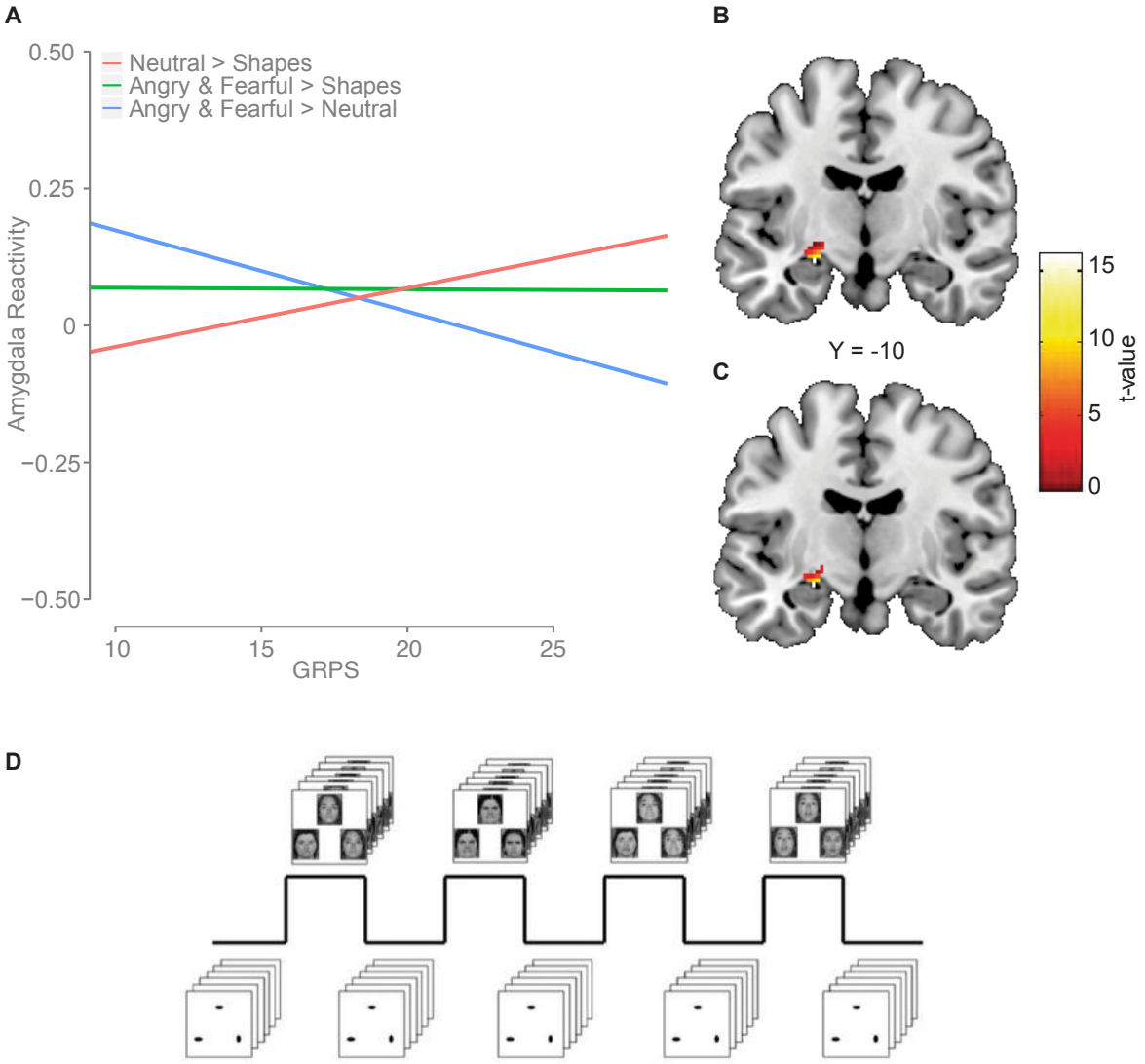

Figure S4. Related to Figure 7.
(A) Elevated genetic risk profile scores (GRPSs) correlate with dysfunctional amygdala reactivity in the entire DNS sample (*n* = 647). As previously found in the European-American subsample, elevated GRPSs predicted blunted amygdala reactivity to threat-related expressions in comparison to neutral expressions in the entire sample when controlling for patterns of population stratification. Post-hoc analyses revealed that GRPS was not predictive of reactivity to threat-related expressions, but that higher GRPSs predicted elevated amygdala reactivity to neutral expressions, in comparison to non-face control stimuli. (B), (C) Show the main effects of the post hoc contrasts for left centromedial amygdala reactivity used in imaging genetics analyses of GRPS in the entire sample. (B) "Angry & Fearful > Shapes" (49 contiguous voxels; max voxel MNI coordinate, x = -24, y = -10, z = -14, t = 22.59, $P < 4.41 \times 10^{-16}$), and (C) "Neutral > Shapes" (35 contiguous voxels; max voxel MNI coordinate, x = -24, y = -10, z = -14, t = 10.73, $P < 4.41 \times 10^{-16}$). (D) DNS fMRI Task: Participants completed four expression-specific (Neutral, Angry, Fear, Surprise) face-matching task blocks interleaved with five sensorimotor shape-matching control blocks. Order for task blocks was counterbalanced across participants.

Table S1. Related to Figure 2.
List of the 320 *cis*-eSNP-probe combinations (*cis*-eQTL bins).

(In separate Excel file.)

Table S2. Related to Figure 5. Overlap of GR-response *cis*-eSNP bin-probe combinations with SNPs nominally associated with MDD in the meta-analysis for MDD (meta-analysis $P \leq 0.05$; $n = 17,846$ samples).
List of 26 eSNP bins (23 tagging SNPs), representing the overlap of the 282 GR-response *cis*-eSNPs and SNPs from the meta-analysis for MDD.

	tag SNP eQTL b	Genes nearby tag SNP	SNP Locati	SNP Chr[a]	PGC A1[b]	PGC A2[c]	PGC OR[d]	PGC RiskA	PGC p-value[f]	P ID[g]	P Gene[h]	Q value[i]	Cross Disorder Association[j]	GR binding site
1	1-148440425	*PLEKHO1, ANP32E*	intergenic	1	T	G	1.09	T	0.013	ILMN_1695435	*HIST2H2AA3/4*	0.006	CDA, BPD, SCZ, ADHD	yes
2	19-40883657	*UPK1A, ZBTB32*	intergenic	19	C	G	0.91	G	0.001	ILMN_1720542	*POLR2I*	0.044	BPD	yes
3	rs10002500	*CNGA1*	intronic	4	T	C	1.07	T	0.043	ILMN_1700306	*OCIAD2*	0.024		no
4	rs10505733	*CLEC4C*	intronic	12	A	C	0.94	C	0.021	ILMN_1665457	*CLEC4C*	0.00021	SCZ	no
	rs10505733	*CLEC4C*	intronic	12	A	C	0.94	C	0.021	ILMN_1682259	*CLEC4C*	0.00021	SCZ	no
5	rs12432242	*SLC7A7*	intronic	14	T	C	0.94	C	0.008	ILMN_1810275	*SLC7A7*	0.041	CDA, BPD	no
6	rs12611262	*SEMA6B, TNFAIP8L1*	intergenic	19	T	C	1.06	T	0.022	ILMN_1658486	*MRPL54*	0.046		no
7	rs12620091	*ALMS1P*	ncRNA_intr	2	T	C	0.95	C	0.022	ILMN_1662954	*CCT7*	0.047		no
8	rs17239727	*BLVRA*	intronic	7	A	G	0.94	G	0.022	ILMN_2081335	*COA1*	0.024	CDA	yes
9	rs1873625	*BSN*	intronic	3	A	C	0.94	C	0.018	ILMN_1705737	*IMPDH2*	0.048		no
10	rs1981294	*LRIF1, DRAM2*	intergenic	1	T	C	1.07	T	0.021	ILMN_1721989	*ATP5F1*	0.037	CDA	no
11	rs2072443	*TMEM176B*	exonic	7	T	C	1.05	T	0.034	ILMN_1791511	*TMEM176A*	0.036		no
12	rs2269799	*SV2B*	intronic	15	T	C	0.95	C	0.04	ILMN_1663699	*SLCO3A1*	0.047		no
13	rs2395891	*BTBD2, MKNK2*	intergenic	19	T	G	1.07	T	0.031	ILMN_1721344	*MOB3A*	0.024	CDA, BPD	yes
	rs2395891	*BTBD2, MKNK2*	intergenic	19	T	G	1.07	T	0.031	ILMN_2347068	*MKNK2*	0.028	CDA, BPD	yes
14	rs2422008	*WDPCP*	intronic	2	A	C	1.05	A	0.036	ILMN_1679268	*PELI1*	0.042	CDA, ASD	yes
15	rs2956993	*GANAB*	intronic	11	T	G	0.95	G	0.032	ILMN_1746525	*FTH1*	0.044		no
16	rs35288741	*NFASC*	intronic	1	A	G	1.05	A	0.042	ILMN_2094952	*NUAK2*	0.044		no
17	rs6493387	*TRPM1*	intronic	15	T	C	0.93	C	0.001	ILMN_1778734	*FAN1*	0.045	CDA	no
18	rs6545924	*COMMD1, B3GNT2*	intergenic	2	T	G	1.06	T	0.018	ILMN_1761242	*COMMD1*	0.045		no
19	rs7194275	*C16orf91, CCDC154*	intergenic	16	T	C	0.92	C	0.021	ILMN_1688749	*RPS2*	0.049	CDA, BPD, SCZ	no
20	rs7252014	*KCNN1*	intronic	19	A	G	1.06	A	0.016	ILMN_1766487	*LRRC25*	0.038		no
21	rs917585	*SLC6A7*	intronic	5	C	G	1.05	C	0.029	ILMN_1694686	*HMGXB3*	0.045	CDA, SCZ	no
22	rs9268671	*HLA-DRA, HLA-DRB5*	intergenic	6	A	G	0.95	G	0.031	ILMN_1697499	*HLA-DRB5*	0.00021	CDA, SCZ, ASD	no
23	rs9268926	*HLA-DRA, HLA-DRB5*	intergenic	6	A	G	0.92	G	0.041	ILMN_1697499	*HLA-DRB5*	0.012	CDA, SCZ, ASD	no
	rs9268926	*HLA-DRA, HLA-DRB5*	intergenic	6	A	G	0.92	G	0.041	ILMN_2159694	*HLA-DRB4*	0.00073	CDA, SCZ, ASD, ADHD	no

[a] *SNP Chromosome*
[b] *code for allele 1 (reference allele, not necessary minor allele)*
[c] *code for allele 2*
[d] *odds ratio*
[f] *risk allele*
[f] *meta analysis p-value*
[g] *Illumina probe identifier (Human HT-12 v3)*
[h] *probe gene*
[i] *lowest Q value for eSNP bin*
[j] *probes that also had an eSNP associated with bipolar disorder (BPD), schizophrenia (SCZ), attention deficit-hyperactivity disorder (ADHD), autism spectrum disorder (ASD) or the cross disorder analysis (CDA)*
[k] *eSNP bins including a GR binding site based on ChIP-seq data*

Table S3. Related to Figure 5. MDD-related GR tagging eSNPs and their proxy SNPs used to generate the cumulative risk allele profile in the MARS cohort. Three SNPs deviated from HWE (rs12620091, rs9268671 and rs9268926) and were excluded from the analysis. As result the remaining 20 SNPs were used to generate a profile.

	tag SNP eQTL bin	Proxy for SNP[a]	Genes nearby tag SNP	SNP Chr	MARS A1[b]	MARS A2[c]	MARS MAF[c]	MARS HWE P value[e]	Used for analysis
1	1-148440425	rs72694971 (renamed)	*PLEKHO1, ANP32E*	1	G	T	0.12	0.56	yes
2	19-40883657	rs73048504 (renamed)	*UPK1A, ZBTB32*	19	C	G	0.18	0.22	yes
3	rs10002500		*CNGA1*	4	T	C	0.13	0.58	yes
4	rs10505733		*CLEC4C*	12	C	A	0.29	0.42	yes
5	rs12432242		*SLC7A7*	14	C	T	0.39	0.87	yes
6	rs12611262		*SEMA6B, TNFAIP8L1*	19	T	C	0.39	0.59	yes
7	rs12620091	rs34874205 (r^2=0.92)	*ALMS1P*	2	C	T	0.37	< 0.00001	no
8	rs17239727		*BLVRA*	7	T	C	0.21	0.48	yes
9	rs1873625		*BSN*	3	A	C	0.29	0.85	yes
10	rs1981294		*LRIF1, DRAM2*	1	C	T	0.17	0.47	yes
11	rs2072443		*TMEM176B*	7	T	C	0.41	0.75	yes
12	rs2269799		*SV2B*	15	C	T	0.32	0.23	yes
13	rs2395891		*BTBD2, MKNK2*	19	T	G	0.35	0.21	yes
14	rs2422008		*WDPCP*	2	A	C	0.43	1	yes
15	rs2956993		*GANAB*	11	G	T	0.38	0.30	yes
16	rs35288741		*NFASC*	1	G	A	0.35	0.25	yes
17	rs6493387		*TRPM1*	15	T	C	0.47	0.11	yes
18	rs6545924		*COMMD1, B3GNT2*	2	G	T	0.50	0.30	yes
19	rs7194275		*C16orf91, CCDC154*	16	C	T	0.12	0.0007	yes
20	rs7252014		*KCNN1*	19	A	G	0.48	0.054	yes
21	rs917585		*SLC6A7*	5	G	C	0.50	0.57	yes
22	rs9268671	rs116072659 (renamed)	*HLA-DRA, HLA-DRB5*	6	A	G	0.34	< 0.00001	no
23	rs9268926	rs114766558 (r^2=0.81)	*HLA-DRA, HLA-DRB5*	6	G	A	0.31	< 0.00001	no

[a] *r^2=LD from MPIP cohort*

[b] *code for allele 1 (reference allele, not necessary minor allele)*

[c] *code for allele 2*

[d] *minor allele frequency*

[e] *Hardy-Weinberg test statistics*

Table S4. Related to Figure 7 and S3. MDD-related GR tagging eSNPs and their proxy SNPs used to generate the cumulative risk allele profile in the DNS cohort. Four SNPs did not have a proxy available (rs12620091, rs917585, rs9268671 and rs9268926). No SNPs deviated from HWE.

							DNS MAF[d]		DNS HWE P values[e]					
	tag SNP eQTL bin	Proxy for SNP[a]	Genes nearby tag SNP	SNP Chr	DNS A1[b]	DNS A2[c]	EUR-AM	ALL	EUR-AM	AFR-AM	Latino/a	Asian1	Asian 2	Used in the analysis
1	1-148440425	rs11588837 (r^2=0.96)	*PLEKHO1, ANP32E*	1	A	G	0.15	0.34	0.48	0.95	0.34	0.99	0.72	yes
2	19-40883657	rs8106959 (r^2=0.95)	KMT2B	19	A	G	0.22	0.18	0.53	0.89	0.87	0.28	0.5	yes
3	rs10002500		*CNGA1*	4	T	C	0.1	0.19	0.28	0.74	0.65	0.48	0.5	yes
4	rs10505733	rs1894823 (r^2=1)	*CLEC4C*	12	T	C	0.31	0.28	0.34	0.4	0.16	0.14	0.35	yes
5	rs12432242	rs2281677 (r^2=0.93)	*SLC7A7*	14	A	G	0.38	0.39	0.96	0.29	0.04	0.16	0.31	yes
6	rs12611262		*SEMA6B, TNFAIP8L1*	19	T	C	0.37	0.44	0.49	0.84	0.57	0.26	0.55	yes
7	rs12620091	no Proxy												no
8	rs17239727	rs10229363 (r^2=1)	*BLVRA*	7	A	G	0.2	0.13	0.23	0.62	0.47	0.86	0.35	yes
9	rs1873625	rs9858280 (r^2=1)	*BSN*	3	T	C	0.37	0.28	0.39	0.6	0.71	0.52	0.24	yes
10	rs1981294	rs4838884 (r^2=1)	*LRIF1, DRAM2*	1	A	G	0.2	0.19	0.63	0.66	0.48	0.932	0.67	yes
11	rs2072443		*TMEM176B*	7	T	C	0.42	0.44	0.38	0.41	0.59	0.39	0.74	yes
12	rs2269799		*SV2B*	15	C	T	0.33	0.35	0.1	0.6	0.32	0.5	0.35	yes
13	rs2395891		*BTBD2, MKNK2*	19	T	G	0.34	0.38	0.49	0.18	0.26	0.3	0.03	yes
14	rs2422008		*WDPCP*	2	A	C	0.47	0.41	0.85	0.25	0.9	0.13	0.82	yes
15	rs2956993		*GANAB*	11	G	T	0.35	0.29	0.42	0.47	0.43	0.61	0.99	yes
16	rs35288741	rs7534993 (r^2=1)	*NFASC*	1	G	A	0.34	0.27	0.24	0.21	0.56	0.53	0.35	yes
17	rs6493387	rs12901022 (r^2=1)	*TRPM1*	15	C	T	0.48	0.46	0.79	0.44	0.41	0.94	0.82	yes
18	rs6545924	rs921320 (r^2=1)	*COMMD1, B3GNT2*	2	C	A	0.5	0.5	0.17	0.53	0.4	0.65	0.94	yes
19	rs7194275		*C16orf91, CCDC154*	16	C	T	0.19	0.19	0.5	0.92	0.73	0.051	1	yes
20	rs7252014		*KCNN1*	19	A	G	0.48	0.47	0.55	0.37	0.31	0.07	0.45	yes
21	rs917585	no Proxy												no
22	rs9268671	no Proxy												no
23	rs9268926	no Proxy												no

[a] *r^2=LD for CEU population from 1KGP (>0.90 for all subpopulations)*

[b] *code for allele 1 (i.e., reference risk allele, not necessary minor allele)*

[c] *code for allele 2*

[d] *minor allele frequencies*

[e] *Hardy-Weinberg test statistics for European Americans (EUR-AM), African Americans (AFR-AM), Latino/as, Asian Cluster 1 (Asian1) and Asian Cluster 2 (Asian2)*

Table S5. Related to Figure 7 and S3. Psychiatric Diagnoses in the Duke Neurogenetics Study (DNS). Of note, this table represents the number of diagnoses across DNS participants. Some individuals presented with a comorbid status.

	European American (*n*=306)	Full Sample (*n*=647)
Alcohol Abuse	22	41
Alcohol Dependence	19	31
Major Depressive Disorder	8	17
Marijuana Abuse	7	15
Gernalized Anxiety Disorder	7	11
Social Anxiety Disorder	3	8
Agoraphobia w/o Panic Disorder	6	8
Bipolar Disorder NOS	6	8
Marijuana Dependence	5	7
Bipolar II	3	6
OCD	4	6
Bulimia Nervosa	2	5
Panic Disorder	1	4
Dysthymia	0	1
PTSD	0	1
Anorexia Nervosa	0	1
Bipolar I	1	1
TOTAL	94	171

Table S6. Related to Figure 2. Sequence of primers used in this study.

List of primers and universal probe library number used for the qPCR for *ADORA3*, *HIST2H2AA3/4* and *TBP* in human whole blood.

Target Gene	Primer Set (5'-3')	UPL probe number
ADORA3	Forward: tcatttgcagccaggtagc	82
	Reverse: tgcttgggtgtggtctatca	
HIST2H2AA3, HIST2H2AA4 (short isoform)	Forward: cgacgaggaactgaacaagc	61
	Reverse: gcctggatgttaggcaagac	
HIST2H2AA3, HIST2H2AA4 (long isoform)	Forward: aaggggcacctgtgaactc	21
	Reverse: gactgagagtggccagcatt	
TBP	Forward: ctttgcagtgacccagcat	67
	Reverse: cgctggaactcgtctcacta	

List of primers used for the qPCR for *LONP1* and *GAPDH* in LCLs.

Target Gene	Primer Set (5'-3')
LONP1	Forward: TTGGTGGCATCAAGGAGAAG
	Reverse: CGGTAGTGTTCCACGAAGTG
GAPDH	Forward: CCAAGGTCATCCATGACAAC
	Reverse: GAGGCAGGGATGATGTTCTG

Oligonucleotides for Chromatin Conformation Capture (3C).

Primer	Sequence
C1	GCCTTACCCAGCACATTTTG
P1	CTGGAAGAGCTTGACCAAGTG
P2	CTCACTCCCCTTGCAATCTC
P3	ACTCGCTTTTTGCAGTAGGG
P4	TACCGCAGCCTACTGCATC
P5	CTTCCACACTGAATCTCACCTG
P6	ATCAATGACCCTCACTCCTCTC
P6	ATCAATGACCCTCACTCCTCTC

Primer set for DNA quantification of 3C samples.

Primer Set (5'-3')
Forward: TGGTGAAACCCCGTCTCTAC
Reverse: AATCTCAGCTCACTGCAACC

SUPPLEMENTAL EXPERIMENTAL PROCEDURES

Samples and study design.

MPIP cohort.

The subject pool for the eQTL analysis consisted of 164 male Caucasian individuals (90% of German origin) recruited for the MARS project (Ising et al., 2009): 93 healthy probands (age = 40.2 ± 12.4 years; body mass index (BMI) = 24.9 ± 3.1 kg/m^2) and 71 in-patients with MDD (age = 48.5 ± 13.5 years; HAM-D = 25.3 ± 8.0; BMI = 26.1 ± 3.6 kg/m^2). All were treated at the hospital of the Max Planck Institute of Psychiatry in Munich, Germany (MPIP; MPIP cohort). Only individuals not reporting a history of current psychiatric, major neurological nor general medical disorders were included in the control sample. Recruitment strategies and further characterization of the MPIP cohort have been described previously (Hennings et al., 2009; Menke et al., 2012). Of these participants, 4 were excluded due genotyping problems.

MARS cohort. This sample included 1,005 MDD patients (561 female, 444 males; age = 48.15 ± 14.13 years; HAM-D = 25.68 ± 6.5), as well as 478 controls (298 females, 180 males; age = 47.83 ± 13.7 years), recruited for the MARS project at the MPIP in Munich, Germany. All included patients were of European descent. Recruitment strategies and further characterization including population stratification of the MARS cohort have been described previously (Hennings et al., 2009; Menke et al., 2012). All individuals used within the eQTL study (MPIP cohort) were not part of this sample.

DNS cohort.

All participants from the Duke Neurogenetics Study (DNS) provided informed written consent, prior to participation, in accord with the guidelines of the Duke University Medical Center Institutional Review Board. All participants were in good general health and free of the following DNS exclusion criteria: (1) medical diagnosis of cancer, stroke, diabetes requiring insulin treatment, chronic kidney or liver disease or lifetime psychotic symptoms; (2) use of psychotropic, glucocorticoid or hypolipidemic medication, and (3) conditions affecting cerebral blood flow and metabolism (e.g., hypertension). Current DSM-IV Axis I and select Axis II disorders (Antisocial Personality Disorder

and Borderline Personality Disorder) were assessed with the electronic Mini International Neuropsychiatric Interview (Sheehan et al., 1998) and Structured Clinical Interview for the DSM-IV Axis II (SCID-II) (First et al., 1997) respectively. These disorders are not exclusionary as the DNS seeks to establish broad variability in multiple behavioral phenotypes related to psychopathology.

On January 6th, 2014, 726 participants had overlapping fMRI and genetic data that was fully processed and used for these analyses. Of these participants, 79 were excluded due to scanner-related artifacts in fMRI data (*n* = 6), incidental structural brain abnormalities (*n* = 2), a large number of movement outliers in fMRI data (*n* = 21; see ART description below), inadequate signal in our amygdala regions of interest (*n* = 14; see coverage description below), poor behavioral performance (*n* = 20; accuracy lower than 75%), outlier status according to ancestrally-informative principal components (*n* = 5), scanner malfunctions (*n* = 2), incomplete fMRI data collection (*n* = 1), and failed genotyping at one GRPS polymorphisms (without a proxy of $r^2 > 0.9$; *n* = 8). Thus, all imaging genetics analyses were conducted in a final European-American subsample of 306 participants (age = 19.72 ± 1.23 years; 148 males; 63 with DSM-IV Axis I disorder) and a full sample of 647 participants (age = 19.65 ± 1.24 years; 285 males; 117 with DSM-IV Axis I disorder; 306 European Americans, 72 African Americans, 170 Asians, 37 Latino/as, and 62 of Other/Multiple racial origins according to self-reported ethnicity; for a full description of diagnoses present in the sample see Table S5).

Mouse models.

The animal experiments were carried out in the animal facilities of the MPIP in Munich, Germany. Male C57BL/6N mice at an age of 12 weeks (mean bodyweight 26.8 ± 0.1 g) were used for the dexamethasone-stimulation test (DEX-mouse). The experiment was performed twice with two separate batches of mice (*n* = 22 per batch). Male 3-4 month old C57BL/6N mice (mean bodyweight 25.5 ± 2.12 g) were used for the acute social defeat mouse model (Stress-mouse). Two weeks before the experiment onset, mice were singly housed and

acclimated to the experimental room. All mice (DEX and Stress-mice) were kept under a 12 h light/dark cycle and standard conditions. Food and tap water were available *ad libitum*. All efforts were made to minimize animal suffering during the experiment. The committee for the Care and Use of Laboratory animals of the Government of Upper Bavaria, Germany approved the protocols.

(i) DEX-mouse: Animals were injected i.p. with either vehicle (VEH, *n* = 11) or 10 mg/kg dexamethasone (DEX, *n* = 11) between 9am and 11am. Animals were sacrificed 4 hours post injection, blood was collected and the brains were carefully removed. The prefrontal cortex (PFC; batch 1), hippocampus (HC; batch 1) and amygdala (AM; batch 2) were dissected immediately according to standard protocols (Spijker, 2011). Amygdala preparation was as follows: brains were cut into ca. 1 mm thick slices using a custom-mounting device. The amygdala (all subnuclei) (Paxinos and Franklin, 2003) was manually dissected with a scalpel under visual control using a binocular microscope. HC and PFC preparation: brain regions were manually dissected from the whole brain by trained personnel. Dissected tissues were directly transferred into RNA lysis solution (Applied Biosystems, USA) and frozen at -80°C. In addition, 300 µl of trunk blood (batch 1) was collected into microcentrifuge tubes containing PaxGene RNA stabilizer solution and frozen at -20°C.

(ii) Stress-mouse: The acute social defeat stress paradigm lasted 5 min and was conducted as previously described (Wagner et al., 2013). Briefly, experimental mice were placed in the home cage of a dominant aggressive CD1 resident mouse. Interaction between the mice was permitted for 5 min without any interference unless an animal was severely injured. When this was the case, the experimental animal was returned to his home cage and excluded from analysis. Prior to the experimental day, all CD1 resident mice received aggression tests to ensure dominance and were trained for aggressive behavior. The control mice were allowed to explore an empty cage (control condition) for 5 min. Exactly 4 h after

the onset of the stress paradigm, the mice were sacrificed and the tissue harvested for subsequent analyses. Briefly, mice were anesthetized with Isofluorane and then immediately killed by decapitation. In the same manner as for the DEX-mouse, 250µl of trunk blood was collected and the brains were carefully removed. The same brain regions i.e. the HC, AM and PFC were dissected out, snap-frozen, and stored in RNA lysis solution at -80°C until needed.

Gene expression data.

Human whole blood of the MPIP cohort was collected using PAXgene Blood RNA Tubes (PreAnalytiX), processed as described previously (Menke et al., 2012) and hybridized to Illumina HumanHT-12 v3.0 Expression Bead Chips. Samples had a mean RNA integrity number (RIN) of 7.97 ± 0.42 *SD*. The Illumina Bead Array Reader was used to scan the microarrays and summarized raw probe intensities were exported using Illumina's GenomeStudio v2011.1 Gene Expression module. Further processing was carried out using R version 2.14.0 (http://www.r-project.org/). All 48,750 probes present on the microarray were first filtered by an Illumina detection *P* value of 0.01 in at least 10% of the samples, leaving 14,168 expressed probes for further analysis. Each transcript was then transformed and normalized through variance stabilization and normalization (VSN) (Lin et al., 2008). Technical batches were adjusted using ComBat with fixed effects of amplification round (Johnson and Cheng, 2007). To test for hidden confounding effects within the ComBat corrected data, we applied a surrogate variable analysis (Leek and Storey, 2007). No significant surrogate variable could be identified suggesting that most of the confounding effects were captured by correcting for known batch effects. To further reduce batch effects baseline and dexamethasone stimulated RNA samples for each individual were processed within a single run. Finally for each probe, we constructed a linear model of the log fold change in gene expression between 6pm (baseline) and 9pm (GR-stimulation) standardized

to 6pm (baseline) controlling for age, disease status and BMI. Models were implemented in "R" using the "lm" function. The residuals (GR-response residuals) from this regression were used as phenotype values in the following analyses. The results did not change when the RIN factor, the dexamethasone serum levels (3 hours following administration) and the differential blood cell count (levels of monocytes, granulocytes and lymphocytes) were included as additional independent covariates.

To control if significant eQTLs might be biased due to SNPs within the probes, the Illumina re-annotation pipeline (ReMOAT version August 2009) (Barbosa-Morais et al., 2010) was used to annotate SNPs (relying on UCSC dbSNP 126 table) that were located within the gene expression probe sequence. No bias of eQTL misclassifications due to such sequence polymorphisms in the probe region could be identified. The probe gene names were updated using the NCBI build 36 (hg18) Reference Sequence (RefSeq) (Pruitt et al., 2012) gene annotation table obtained from the UCSC Table Browser (http://hgdownload.soe.ucsc.edu/goldenPath/hg18/database/refGene.txt.gz). The positions of the probes were annotated using ReMOAT and only autosomal probes were used for the GR-response eQTL analysis (n = 4,447 autosomal probes).

DEX-mouse und Stress-mouse RNA was extracted from whole blood using the PAXgene blood miRNA kit (PreAnalytiX) according to (Krawiec et al., 2009). RNA was extracted from the mouse brain regions using RNeasy Plus Universal Mini Kit (Qiagen) in the DEX-mouse experiment and using TRIzol (Life Technologies) in the Stress-mouse experiment, both according to manufacturer's protocol. RNA was quality checked using the Agilent 2100 Bioanalyser, amplified using the Illumina Total Prep 96-Amplification kit (Life Technology) and then hybridized on Illumina MouseRef-8 v2.0 (for DEX-mouse) and Illumina MouseWG-6 v2.0 BeadChips (for Stress-mouse). For each tissue and experiment the samples were processed together (RNA amplification, hybridization and scanning). All samples had a mean RIN of 7.5 ± 0.2 *SD* for DEX-mouse and 6.6 ± 0.5 *SD* for Stress-mouse

blood cells and a mean RIN of 9.2 ± 0.4 *SD* for DEX-mouse and 9.2 ± 0.3 *SD* Stress-mouse brain tissues. All probes present on the microarrays (MouseRef-8 = 25,700; MouseWG-6 = 45,200 probes) were first filtered using an Illumina detection *P* value of 0.05 in at least 15% of the samples. Secondly, each transcript was transformed, normalized and batch corrected, in the same fashion as for the human gene expression data. For differential gene expression analysis between the VEH and DEX animals, as well as between control and stress animals linear regression models implemented in R were used on the normalized, transformed and batch corrected expression values for each tissue. Multiple testing corrections were performed by controlling the false discovery rate (*FDR*) according to Benjamini and Hochberg. A *FDR* ≤ 10% was considered as significant. Results were illustrated as a heatmap in Figure 6B. If multiple array probes per gene existed, only the most significant one is shown in Figure 6B.

Genotype data.

Human DNA of the MPIP cohort samples was isolated from EDTA blood samples using the Gentra Puregene Blood Kit (Qiagen) with standardized protocols. Genome-wide SNP genotyping was performed using Illumina Human610-Quad and Illumina Human660W-Quad Genotyping BeadChips according to the manufacturer's standard protocols. In total, 582,539 genetic markers in 163 individuals of the MPIP cohort could be successfully genotyped. Individuals with low genotyping rate (<98%) and SNPs showing significant deviation from the Hardy-Weinberg equilibrium (HWE, *P* value < 1×10^{-5}) were excluded. Similarly, a low minor allele frequency (MAF;<10%) and SNPs with high rates of missing data (>2%) were excluded. This resulted in 436,643 SNPs and 160 individuals for further analysis. In the 160 samples that passed the quality control, imputation of additional variants was performed using IMPUTE v2 (Howie et al., 2009) on the basis of HapMap CEU Phase 3 (International HapMap Consortium, 2003) and 1,000 Genomes Project version June 2010 (hg18) CEU

data for ~8 million SNPs (Durbin et al., 2010). Imputed SNPs were excluded if their posterior probability averages were less than 90% for the most likely imputed genotype (INFO ≥ 0.9). SNPs were also excluded if their call rate was less than 98%, HWE *P* value was less than 1×10^{-5} and MAF < 10%. This yielded a total of 2,011,895 SNPs. To annotate SNPs for the closest gene, we used Annovar version November 2011 (Wang et al., 2010) with the RefSeq gene annotation SNP coordinates are given according to hg18.

Human DNA of the MARS cohort samples was extracted from EDTA blood samples using the Gentra Puregene Blood Kit (Qiagen) with standardized protocols. Whole-genome SNP genotyping was performed on Illumina Sentix Human-1, HumanHap300, Human610-Quad and HumanOmniExpress Genotyping BeadChips according to the manufacturer's standard protocols. Individuals as well as the genotype data have been subjected to the same quality control steps as the MPIP cohort (genotyping rate < 98%, MAF < 10%, HWE *P* value < 1×10^{-5}, SNP missingness < 98%). Missing genotype data were imputed via IMPUTE v2 based on the 1,000 Genomes Project version Nov. 2010 ALL reference panel. The MDD-related GR eSNP profile was derived from loci associated with both dexamethasone-induced differences in gene expression and MDD. It included alleles from 20 of the 23 tag eSNPs (3 SNPs diverged from HWE in the MARS sample, Table S3. Non-risk and risk alleles (according to association with depression in the PGC dataset) were coded 0 and 1, respectively, and summed in an additive fashion to create cumulative genetic risk profile scores (GRPS; 0 ,1 ,2). The MARS GRPSs ranged from 12-30.

Human DNA from participants of the DNS cohort was isolated from saliva derived from Oragene DNA self-collection kits (DNA Genotek) customized for 23andMe. DNA extraction and genotyping were performed by the National Genetics Institute (NGI), a CLIA-certified clinical laboratory and subsidiary of Laboratory Corporation of America. The Illumina HumanOmniExpress BeadChips and a custom array containing an additional ~300,000 SNPs were used to provide genome-wide data. Due to differences in genotyping array

content the DNS GRPSs included alleles from 19 of the 23 eSNPs (Table S4) and were coded in the same way as the MARS GRPSs. All SNPs used for the GRPSs had genotyping rates < 97%, MAF < 10%, HWE *P* value < 1×10^{-5} (Table S4). DNS GRPSs ranged from 10-28 and were normally distributed (Figure 7). To account for differences in ancestral background in the full sample, we used EIGENSTRAT (v, 5.0.1) (Price et al., 2006) to generate principal components and included the first 5 components as covariates in the analysis. Five participants were outliers for these components (± 6 *SD* from the mean on one of the top ten components) and hence were excluded from analyses.

DNS neuroimaging protocol.

*BOLD fMRI paradigm***.**

A widely used and reliable challenge paradigm was employed to elicit amygdala reactivity. The paradigm consists of 4 task blocks requiring face-matching interleaved with 5 control blocks requiring shape-matching (see Figure S4D). In each face-matching trial within a block, participants view a trio of faces derived from a standard set of facial affect pictures (expressing angry, fearful, surprised, or neutral emotions), and select which of the 2 faces presented on the bottom row of the display matches the target stimulus presented on the top row. Each emotion-specific block (e.g., fearful facial expressions only) consists of 6 individual trials, balanced for gender of the face. Block order is pseudo-randomized across participants. Each of the 6 face trios is presented for 4 seconds with a variable inter-stimulus interval of 2-6 seconds; total block length is 48 seconds. In the shape-matching control blocks, participants view a trio of geometric shapes (i.e., circles, horizontal and vertical ellipses) and select which of 2 shapes displayed on the bottom matches the target shape presented on top. Each control block consists of 6 different shape trios presented for 4 seconds with a fixed inter-stimulus interval of 2 seconds, comprising a total block length of 36 seconds. The total paradigm was 390 seconds in duration. Reaction times and accuracy are recorded through an MR-compatible button box.

BOLD fMRI acquisition.

Participants were scanned using a research-dedicated GE MR750 3T scanner equipped with high-power high-duty-cycle 50-mT/m gradients at 200 T/m/s slew rate, and an eight-channel head coil for parallel imaging at high bandwidth up to 1MHz at the Duke-UNC Brain Imaging and Analysis Center. A semi-automated high-order shimming program was used to ensure global field homogeneity. A series of 34 interleaved axial functional slices aligned with the anterior commissure-posterior commissure (AC-PC) plane were acquired for full-brain coverage using an inverse-spiral pulse sequence to reduce susceptibility artifact (TR/TE/flip angle = 2000 ms / 30 ms / 60; FOV = 240 mm; 3.75 × 3.75 × 4 mm voxels (selected to provide whole brain coverage while maintaining adequate signal-to-noise and optimizing acquisition times); interslice skip = 0). Four initial RF excitations were performed (and discarded) to achieve steady-state equilibrium. To allow for spatial registration of each participant's data to a standard coordinate system, high-resolution three-dimensional structural images were acquired in 34 axial slices co-planar with the functional scans (TR/TE/flip angle = 7.7s / 3.0 ms / 12; voxel size = 0.9 × 0.9 × 4 mm; FOV = 240 mm; interslice skip = 0).

BOLD fMRI data analysis.

The general linear model of Statistical Parametric Mapping 8 (SPM8) (http://www.fil.ion.ucl.ac.uk/spm) was used for whole-brain image analysis. Individual subject data were first realigned to the first volume in the time series to correct for head motion before being spatially normalized into the standard stereotactic space of the Montreal Neurological Institute (MNI) template using a 12-parameter affine model. Next, data were smoothed to minimize noise and residual differences in individual anatomy with a 6mm FWHM Gaussian filter. Voxel-wise signal intensities were ratio normalized to the whole-brain global mean. Then the ARTifact Detection Tool (ART; https://www.nitrc.org/docman/view.php/104/390/Artifact%20Detection%20Toolbox%20Manu

al) was used to generate regressors accounting for images due to large motion (i.e., > 0.6 mm relative to the previous time frame) or spikes (i.e., global mean intensity 2.5 standard deviations from the entire time series). Participants for whom more than 5% of acquisition volumes were flagged by ART (*n* = 21) were removed from analyses. An region of interest (ROI) mask (Automated Anatomical Labeling (AAL) atlas) from WFU pickatlas (Maldjian et al., 2003) was used to ensure adequate amygdala coverage for the face-matching and number-guessing tasks, respectively. Participants who had less than 90% coverage of the amygdala (*n* = 14) were excluded from analyses.

Following preprocessing steps outlined above, linear contrasts employing canonical hemodynamic response functions were used to estimate task-specific (i.e., "Angry & Fearful Faces > Neutral Faces", "Angry & Fearful > Shapes", "Neutral > Shapes") BOLD responses for each individual. The primary contrast of "Angry & Fearful > Neutral" was used to assay centromedial reactivity to cues that are conditioned social signals to threat in the environment (i.e., angry and fearful expressions) relative to signals that do not convey threat information about the environment (i.e., neutral expressions). Post-hoc analyses using the "Angry & Fearful > Shapes" and "Neutral > Shapes" contrasts were used to discern if the association with GRPS reflected relatively decreased reactivity to angry and fearful expressions or increased reactivity to neutral expressions. Individual contrast images (i.e., weighted sum of the beta images) were used in second-level random effects models accounting for scan-to-scan and participant-to-participant variability to determine mean contrast-specific responses using one-sample t-tests. A voxel-level statistical threshold of *P* value < 0.05, family wise error corrected for multiple comparisons across the bilateral centromedial amygdala ROIs, and a cluster-level extent threshold of 10 contiguous voxels was applied to these analyses. The bilateral centromedial amygdala ROIs were defined using anatomical probability maps (Amunts et al., 2005). The centromedial ROI was chosen because it includes the central nucleus of the amygdala (CeA). This specifically functions to drive physiologic, attentive, and

neuromodulatory responses to threat, as opposed to the basolateral complex of the amygdala (BLA), which primarily functions to relay information to the CeA. Thus, the expression of stress responsive behavior is more closely linked with the activity of the CeA and not the BLA (Davis and Whalen, 2001; LeDoux, 2007). Human research using such distinctions has shown that ROIs encompassing the CeA or BLA differentially respond to stimuli and share different patterns of functional as well as structural connectivity (Brown et al., 2014; Etkin et al., 2004; Lerner et al., 2012).

BOLD parameter estimates from a cluster within the left centromedial amygdala ROI exhibiting a main effect for the "Angry & Fearful > Neutral" contrast were extracted using the VOI tool in SPM8 and exported for regression analyses in SPSS (v.18). No significant cluster emerged in the right centromedial amygdala. Extracting parameter estimates from clusters activated by our fMRI paradigm, rather than those specifically correlated with our independent variables of interest, precludes the possibility of any correlation coefficient inflation that may result when an explanatory covariate is used to select a region of interest. We have successfully used this strategy in prior studies (Bogdan et al., 2012).

Statistical Analysis.

Cis-associations of baseline gene expression.

Using baseline gene expression of the 4,447 differently regulated autosomal array probes (absolute fold change ≥ 1.3 in at least 20% of all samples), 26,205 unique *cis*-SNPs and 764 gene expression probes corresponding to 31,541 *cis*-eQTLs were found to be significant after multiple testing correction with the same strategy as described for the GR-stimulated gene expression changes. The 26,205 unique eSNPs represented 1,010 uncorrelated eSNP bins (1,148 eSNP bin-probe combinations). The 775 eQTL bins (68%) were located within 100 kb upstream or downstream from the array probe ends, 911 eQTL bins (79%) within 200 kb and only 237 eQTLs bins > 200 kb (21%).

Validation GR-response cis-eQTL results

Validation of GR-response *cis*-eQTL results was carried out with a sample size-weighted Z-score meta-analysis (Evangelou and Ioannidis, 2013) in an additional independent data set using peripheral blood samples (baseline and after GR-stimulation with 1.5 mg dexamethasone) of 58 individuals (21 male controls, 14 male cases and 23 female cases). We applied the same strategy as used in the discovery sample (MPIP cohort) to filter, normalize and batch correct the gene expression data. We adjusted the analysis for the same covariates plus gender; applied the same SNP quality control checks and performed the *cis*-eQTL mapping in PLINK.

Enrichment of GR binding regions

To identify whether GR-response eSNPs were enriched for GR binding sites, we used the *E*NCODE (ENCODE Project Consortium, 2011) *NR3C1* ChIP-seq data from GM12878 LCLs (accession: ENCSR904YPP) from which no aligned tracks are currently available. Raw data were download at https://www.encodeproject.org/experiments and initial filtering was performed using FASTX Toolkit (v. 0.0.14, http://hannonlab.cshl.edu/fastx_toolkit/index.html) and Prinseq (v. 0.20.3) (Schmieder and Edwards, 2011) to eliminate artifacts and low quality reads. Alignment on hg19 was performed using BWA (v. 0.7.10) (Li and Durbin, 2009) allowing only uniquely mappable alignments with alignment quality of above 20. Reads from both ChIP and both control libraries were pooled leading to 46,453,650 and 68,227,580 used reads, respectively. Peak-calling was carried out by MACS14 (v. 1.4.2) (Zhang et al., 2008) using default settings, resulting in around 23,000 annotated signals. The average length of a ChIP signal as defined by the peak calling was 746.3 bps ± 370.6 bsp.

We mapped the GR-response eSNPs to these GR ChIP-seq peaks and compared the overlap observed with 1,000 equal sized sets of randomly drawn SNPs (n=3,662 SNPs) from of all analyzed SNPs (without replacement) matched in MAF (=null distribution). To match the MAF distributions of the random SNP sets with our GR-response eQTL data we

divided the SNPs into non-overlapping MAF bins, each of the width 0.05 as described previously (Nicolae et al., 2010). For every set we counted the percentage of SNPs within a GR ChIP-seq peak. Enrichment calculations with a permutation-based *FDR* < 10% were considered as statistically significant within the entire manuscript.

Enhancer enrichment analysis

We investigated whether GR-response eSNP binds are enriched for functional enhancer annotations using the online tool HaploReg version 2 (Ward and Kellis, 2012) based on the Roadmap Epigenome data (Roadmap Epigenomics Consortium et al., 2015) and using the 1,000 Genomes Project CEU data as a background data set. Additionally we performed the enrichment analysis on ten permuted baseline eSNP bin sets (size matched) to generate a realistic null distribution. The average enhancer enrichment over the ten permutations is present in Figure 3 and S2.

Chromatin interaction analysis with paired-end tag (ChIA-PET) mapping.

The combined set of the first two replicates of the RNA Polymerase II ChIA-PET data (Li et al., 2010; 2012) generated from K562 chronic myeloid leukemia cell lines (*n* > 400,000 interaction regions) was obtained from the UCSC Genome Browser (http://hgdownload.cse.ucsc.edu/goldenPath/hg19/encodeDCC/wgEncodeGisChiaPet/). Genomic coordinates of our GR-response eSNP bins were converted from hg18 to GRCh build 37 (hg19) using the UCSC Genome Browser liftOver tool (http://genome.ucsc.edu/cgi-bin/hgLiftOver) and the probe gene coordinates were updated with the hg19 RefSeq (Pruitt et al., 2012) gene table obtained from the UCSC Table Browser (http://hgdownload.soe.ucsc.edu/goldenPath/hg19/database/refGene.txt.gz; excluding 15 probe genes on hg19). To estimate the overlap of the direct chromatin interactions and GR-response eQTL bins (eSNP bin-probe gene combination) we tested if one ChIA-PET tag overlapped with the region of the eSNP bin ± 10kb as well as the relevant array probe gene

(10kb ± transcription start or end). To establish the null distribution, we permuted the distances between the GR-response eSNP bins and the transcription sites of the corresponding probe gene (*n* = 270 updated to hg19) and estimated the overlap with ChIA-PET interaction signals. We repeated the analysis 1,000 times and for each set we counted the number of genes with overlapping ChIA-PET data.

Enrichment of GWAS susceptibility markers.

To identify whether GR-response eSNPs were specifically enriched for association with psychiatric disorders and not with other diseases or traits, we generated 1,000 sets of permuted baseline eSNPs (conditional on MAF and number of GR-response eSNPs overlapping with the respective GWAS). For every set we counted the percentage of unique SNPs with a GWAS results at *P* value ≤ 0.05. On this basis we constructed the null distribution. A second null distribution was created based on all imputed SNPs of high quality.

1.) PGC MDD data: The MDD GWAS data was generated by conducting a meta-analysis based on the Psychiatric Genomics Consortium (PGC) GWAS mega-analysis for MDD (Major Depressive Disorder Working Group of the Psychiatric GWAS Consortium, 2012) data . We used the “meta-analysis” function in PLINK assuming a fixed effect model in 17,846 individuals of European ancestry (8,864 cases with MDD and 8,982 controls) from 8 of the 9 studies included in the PGC MDD data. All samples from the initial PGC MDD data (*n* = 18,759) that overlapped with our MARS cohort (*n* = 376 cases and 537 controls) were excluded, which was then used as validation sample. The PGC MDD analysis used SNP data imputed to the 1,000 Genomes Project (hg19).

2.) PGC cross-disorder data: The results of the PGC cross-disorder (CD) analysis (33,332 patients and 27,888 controls of European ancestry distributed among five disorders: SCZ, BPD, ADHD, ASD and MDD) (Cross-Disorder Group of the Psychiatric Genomics

Consortium, 2013; Cross-Disorder Group of the Psychiatric Genomics Consortium et al., 2013) were obtained from the PGC website (http://pgc.unc.edu). The PGC CD analysis applied a multinomial regression procedure and used SNP data imputed to the HapMap Phase 3 data (hg18).

3.) PGC SCZ2 data: The results of the multistage GWAS for SCZ (Schizophrenia Working Group of the Psychiatric Genomics, 2014) obtained from the PGC website (http://pgc.unc.edu). The PGC SCZ2 analysis used SNP data imputed to the 1,000 Genomes Project (hg19).

4.) Non psychiatric trait data: The GWAS data for height (Heid et al., 2010) and rheumatoid arthritis (RA) (Stahl et al., 2010) were obtained from the PGC website (http://pgc.unc.edu). Results of the Crohn's disease (CD) analysis were obtained from International Inflammatory Bowel Disease Genetics Consortium website (http://www.ibdgenetics.org). The RA analysis used SNP data imputed to the HapMap Phase 2 data (hg17) and the CD as well as height data was imputed based on HapMap Phase 3. For comparability we converted all our SNP coordinates to the relevant genome assembly of analyzed GWAS data using the UCSC Genome Browser liftOver tool.

Co-expression analysis

For the co-expression analysis we used the GR-response residuals from all array probes (*n* = 4,447) to determine if the 25 MDD-related GR array probes are more co-regulated than 1,000 sets of randomly chosen GR-stimulated transcripts. To realize this, we carried out a co-expression analysis in R using the function "dist" specifying the Euclidian distance as distance measure and calculated the mean distance of all pair-wise distances. We established the significance of co-expression network of the 25 MDD-related GR array probes by testing the observed mean distance versus the null distributions created by

calculating the mean distance of all pair-wise distances for 1,000 sets of 25 randomly chosen GR-stimulated transcripts. Next, we determined the number of sets, having lower mean distances than the actual MDD-related GR transcripts to measure the enrichment statistic.

*DNS neuroimaging analysis***.**

Statistical analyses of the imaging data were completed using linear regression in SPSS to test the association of the MDD-related GR tag eSNP GRPSs to amygdala reactivity in the independent DNS cohort. To maintain variability but constrain the influence of extreme outliers, prior to any analyses, all imaging variables were winsorized (i.e., following data quality control procedures, outliers more than ± 3 SD were set at ± 3 SD from the mean; for the "Angry and Fearful > Neutral faces" contrast, 13 outliers (2.01%) of the entire sample were moved to ± 3 SD from the mean). Gender, psychiatric diagnosis (0,1) and age were entered as covariates for both EUR-AM and entire sample analyses. Five ancestrally-informative principal components that distinguish the sample were added as additional covariates in the analyses of the entire sample. We computed permutations (n = 1,000) in which we constructed randomly generated SNP profiles that were matched for MAF, amount of SNPs (n = 19) and constrained by the max LD observed within the sample.

Graphs were generated with Haploview (Barrett et al., 2005), ggplot2 ((Wickham, 2009) and Circos (Krzywinski et al., 2009).

Chromatin conformation capture

Five human lymphoblastoid cell lines were cultured in RMPI media with stable l-glutamine (Biochrom) supplemented with 10% fetal bovine serum and 1% antibiotic-antimycotic (Life Technologies). Crosslinking and cell lysis were performed as described (Hagège et al., 2007). Nuclei were digested using 1,000 U of *Nco*I. Subsequent re-ligation, de-crosslinking and purification were conducted according to the manufacturer's protocol. Following assessment of digestion efficiency and sample purity, DNA concentration of the 3C samples

were determined by SybrGreen quantitative PCR using an “internal” primer set (see Table S6; primers that do not amplify across sites recognized by the restriction enzyme used) as described in (Hagège et al., 2007). Primers were designed with an anchor primer in the fragment containing the TSS of *LONP1* and in potential interacting fragments in and around eSNP bin of *NRTN* using Primer3Plus (http://www.bioinformatics.nl/cgi-bin/primer3plus/primer3plus.cgi). Quantitative PCR was carried out using ABsolute Blue qPCR SYBR Green Master Mix (Thermo Fisher Scientific) and the Mini Opticon Real-Time PCR System (Bio-Rad) according to the manufacturer’s instructions. A 179-kb BAC clone (CTD-2522A4) containing the entire *LONP1-NRTN* genomic sequence was purchased from Life Technologies and served as PCR control template. The BAC clone was cut with *Nco*I and re-ligated by T4 DNA ligase. All primer pairs were tested on a standard curve of the BAC control library and yielded PCR efficiencies > 1.7. The presence of a single PCR product was confirmed by agarose gel electrophoresis and melting curve analysis. Cycling conditions were: 95 °C for 15min, 45 cycles of 95°C for 15s, 60°C for 15s, 72°C for 15s. Quantitative PCR data were normalized to *GAPDH* as a loading control. *GAPDH* cycling conditions were 95 °C for 15min, 45 cycles of 95°C for 15s, 60°C for 15s, 72°C for 15s. Data analysis was carried out according to (Hagège et al., 2007) and is presented as relative crosslinking frequency. Primers used for the chromatin conformation capture interaction studies are listed in Table S6. Linear mixed models were used for statistical analysis.

Quantitative real-time PCR (qPCR) validation.

Total RNA was reverse-transcribed to cDNA using random primers and the Superscript II reverse transcriptase (Invitrogen) for qPCR to validate microarray results. qPCR was carried out according to manufactures instructions using Roche-LightCycler 480 System (Roche Applied Science) and assays were designed using the Roche Universal Probe Library (http://qpcr.probefinder.com) for *ADORA3* (the probe with a significant GR-response eQTLs), *HIST2H2AA3/4* (the probe with the most eSNPs overlapping with the meta-analysis results

for MDD) and *TBP* as the endogenous control gene. Assays for *LONP1* and *GADPH* were designed using Primer3Plus (http://www.bioinformatics.nl/cgi-bin/primer3plus/primer3plus.cgi). The association between eSNPs and GR-stimulated gene expression of the target genes could be validated using qPCR (see Figure 2C,D and 4A,B). Sequences of primers used are summarized in Table S6. All samples were run in duplicates and duplicates discordant in *CT* values by more than 0.2 cycles, were excluded from the analysis. Relative gene transcript levels were determined by Pfaffl's equation (Pfaffl, 2001) with: $\text{ratio} = \frac{(\text{E}_{\text{gene}})^{\Delta\text{CT}_{\text{gene}}(\text{baseline sample} - GR-\text{stimulated sample})}}{(\text{E}_{\text{housekeeper}})^{\Delta\text{CT}_{\text{housekeeper}}(\text{baseline sample} - GR-\text{stimulated sample})}}$. qPCR ratios shown in Figure 2D and were calculated using the following equations:

$$pre = \frac{(E_{housekeeper})^{CT_{housekeeper}(baseline\ sample)}}{(E_{gene})^{CT_{gene}(baseline\ sample)}}$$

and *post* = $\frac{(E_{housekeeper})^{CT_{housekeeper}(GR-stimulated\ sample)}}{(E_{gene})^{CT_{gene}(GR-stimulated\ sample)}}$.

qPCR validation results.

Two transcript variants encoding isoforms with a different 3'UTR length have been identified for *HIST2H2AA3/4*. The shorter gene product (isoform 1) is annotated by RefSeq while the alternatively spliced longer gene product (isoform 2) is annotated by Ensembl release 54 (HIST2H2AA3-001; ENST00000369161) and further predicted by AceView (HIST2H2AA3.aApr07-unspliced, HIST2H2AA4.aApr07-unspliced). This longer isoform is tagged by the significant Illumina probe (ILMN_1695435). Hence we designed two different assays- one covering the common part of both isoforms (assay 1) and the other tagging isoform 2 (assay 2). The expression levels measured with both assays were highly correlated (Spearman's test *P* value < 1.5×10^{-20}, *R* = 74%). We could replicate a significant SNP effect in 137 samples with a *P* value of 0.012 using assay 1 with a genotypic model and *P* = 0.017 using a carrier model, with the same direction of change as in the expression array.

SUPPLEMENTAL REFERENCES

Amunts, K., Kedo, O., Kindler, M., Pieperhoff, P., Mohlberg, H., Shah, N.J., Habel, U., Schneider, F., and Zilles, K. (2005). Cytoarchitectonic mapping of the human amygdala, hippocampal region and entorhinal cortex: intersubject variability and probability maps. Anat. Embryol. *210*, 343–352.

Barbosa-Morais, N.L., Dunning, M.J., Samarajiwa, A.S., Darot, J.F.J., Ritchie, M.E., Lynch, A.G., and Tavaré, S. (2010). A re-annotation pipeline for Illumina BeadArrays: improving the interpretation of gene expression data. Nucleic Acids Res. *38*, e17.

Barrett, J.C., Fry, B., Maller, J., and Daly, M.J. (2005). Haploview: analysis and visualization of LD and haplotype maps. Bioinformatics *21*, 263–265.

Bogdan, R., Williamson, D.E., and Hariri, A.R. (2012). Mineralocorticoid receptor Iso/Val (rs5522) genotype moderates the association between previous childhood emotional neglect and amygdala reactivity. Am J Psychiat *169*, 515–522.

Brown, V.M., Labar, K.S., Haswell, C.C., Gold, A.L., McCarthy, G., Morey, R.A., and Workgrp, M.-A.M. (2014). Altered Resting-State Functional Connectivity of Basolateral and Centromedial Amygdala Complexes in Posttraumatic Stress Disorder. Neuropsychopharmacology *39*, 351–359.

Cross-Disorder Group of the Psychiatric Genomics Consortium (2013). Identification of risk loci with shared effects on five major psychiatric disorders: a genome-wide analysis. The Lancet *381*, 1371–1379.

Cross-Disorder Group of the Psychiatric Genomics Consortium, Lee, S.H., Ripke, S., Neale, B.M., Faraone, S.V., Purcell, S.M., Perlis, R.H., Mowry, B.J., Thapar, A., Goddard, M.E., et al. (2013). Genetic relationship between five psychiatric disorders estimated from genome-wide SNPs. Nat Genet *45*, 984–994.

Davis, M., and Whalen, P.J. (2001). The amygdala: vigilance and emotion. Molecular Psychiatry *6*, 13–34.

Durbin, R.M., Altshuler, D.L., Durbin, R.M., Abecasis, G.R., Bentley, D.R., Chakravarti, A., Clark, A.G., Collins, F.S., La Vega, De, F.M., Donnelly, P., et al. (2010). A map of human genome variation from population-scale sequencing. Nature *467*, 1061–1073.

ENCODE Project Consortium (2011). A user's guide to the encyclopedia of DNA elements (ENCODE). PLoS Biol. *9*, e1001046.

Etkin, A., Klemenhagen, K.C., Dudman, J.T., Rogan, M.T., Hen, R., Kandel, E.R., and Hirsch, J. (2004). Individual differences in trait anxiety predict the response of the basolateral amygdala to unconsciously processed fearful faces. Neuron *44*, 1043–1055.

Evangelou, E., and Ioannidis, J.P.A. (2013). Meta-analysis methods for genome-wide association studies and beyond. Nature Reviews Genetics *14*, 379–389.

First, M.B., Gibbon, M., Spitzer, R.L., Williams, J.W.B., and Benjamin, L.S. (1997). Structured Clinical Interview for DSM-IV Axis II Personality Disorders, (SCID-II). Washington, D.C.: American Psychiatric Press, Inc.

Hagège, H., Klous, P., Braem, C., Splinter, E., Dekker, J., Cathala, G., de Laat, W., and Forné, T. (2007). Quantitative analysis of chromosome conformation capture assays (3C-qPCR). Nat Protoc *2*, 1722–1733.

Heid, I.M., Jackson, A.U., Randall, J.C., Winkler, T.W., Qi, L., Steinthorsdottir, V., Thorleifsson, G., Zillikens, M.C., Speliotes, E.K., Mägi, R., et al. (2010). Meta-analysis identifies 13 new loci associated with waist-hip ratio and reveals sexual dimorphism in the genetic basis of fat distribution. Nat Genet *42*, 949–960.

Hennings, J.M., Owashi, T., Binder, E.B., Horstmann, S., Menke, A., Kloiber, S., Dose, T., Wollweber, B., Spieler, D., Messer, T., et al. (2009). Clinical characteristics and treatment outcome in a representative sample of depressed inpatients-findings from the Munich Antidepressant Response Signature (MARS) project. J Psychiatr Res *43*, 215–229.

Howie, B.N., Donnelly, P., and Marchini, J. (2009). A flexible and accurate genotype imputation method for the next generation of genome-wide association studies. PLoS Genet *5*, e1000529.

International HapMap Consortium (2003). The International HapMap Project. Nature *426*, 789–796.

Ising, M., Lucae, S., Binder, E.B., Bettecken, T., Uhr, M., Ripke, S., Kohli, M.A., Hennings, J.M., Horstmann, S., Kloiber, S., et al. (2009). A genomewide association study points to multiple loci that predict antidepressant drug treatment outcome in depression. Archives of General Psychiatry *66*, 966–975.

Johnson, W.E., and Cheng, L. (2007). Adjusting batch effects in microarray expression datausing empirical Bayes methods. Biostatistics *8*, 118–127.

Krawiec, J.A., Chen, H., Alom-Ruiz, S., and Jaye, M. (2009). Modified PAXgene (TM) method allows for isolation of high-integrity total RNA from microlitre volumes of mouse whole blood. Lab. Anim. *43*, 394–398.

Krzywinski, M., Schein, J., Birol, I., Connors, J., Gascoyne, R., Horsman, D., Jones, S.J., and Marra, M.A. (2009). Circos: an information aesthetic for comparative genomics. Genome Research *19*, 1639–1645.

LeDoux, J. (2007). The amygdala. Curr. Biol. *17*, R868–R874.

Leek, J.T., and Storey, J.D. (2007). Capturing heterogeneity in gene expression studies by surrogate variable analysis. PLoS Genet *3*, 1724–1735.

Lerner, Y., Singer, N., Gonen, T., Weintraub, Y., Cohen, O., Rubin, N., Ungerleider, L.G., and Hendler, T. (2012). Feeling without Seeing? Engagement of Ventral, but Not Dorsal, Amygdala during Unaware Exposure to Emotional Faces. Journal of Cognitive Neuroscience *24*, 531–542.

Li, G., Fullwood, M.J., Xu, H., Mulawadi, F.H., Velkov, S., Vega, V., Ariyaratne, P.N., Mohamed, Y.B., Ooi, H.-S., Tennakoon, C., et al. (2010). ChIA-PET tool for comprehensive chromatin interaction analysis with paired-end tag sequencing. Genome Biol *11*, R22.

Li, G., Ruan, X., Auerbach, R.K., Sandhu, K.S., Zheng, M., Wang, P., Poh, H.M., Goh, Y., Lim, J., Zhang, J., et al. (2012). Extensive promoter-centered chromatin interactions provide

a topological basis for transcription regulation. Cell *148*, 84–98.

Li, H., and Durbin, R. (2009). Fast and accurate short read alignment with Burrows-Wheeler transform. Bioinformatics *25*, 1754–1760.

Lin, S.M., Du, P., Huber, W., and Kibbe, W.A. (2008). Model-based variance-stabilizing transformation for Illumina microarray data. Nucleic Acids Res. *36*, e11.

Major Depressive Disorder Working Group of the Psychiatric GWAS Consortium (2012). A mega-analysis of genome-wide association studies for major depressive disorder. Molecular Psychiatry *18*, 497–511.

Maldjian, J.A., Laurienti, P.J., Kraft, R.A., and Burdette, J.H. (2003). An automated method for neuroanatomic and cytoarchitectonic atlas-based interrogation of fMRI data sets. Neuroimage *19*, 1233–1239.

Menke, A., Arloth, J., Pütz, B., Weber, P., Klengel, T., Mehta, D., Gonik, M., Rex-Haffner, M., Rubel, J., Uhr, M., et al. (2012). Dexamethasone Stimulated Gene Expression in Peripheral Blood is a Sensitive Marker for Glucocorticoid Receptor Resistance in Depressed Patients. Neuropsychopharmacology *37*, 1455–1464.

Nicolae, D.L., Gamazon, E., Zhang, W., Duan, S., Dolan, M.E., and Cox, N.J. (2010). Trait-associated SNPs are more likely to be eQTLs: annotation to enhance discovery from GWAS. PLoS Genet *6*, e1000888.

Paxinos, G., and Franklin, K.B.J. (2003). The mouse brain in stereotaxic coordinates. Academic Press; 2 Edition.

Pfaffl, M.W. (2001). A new mathematical model for relative quantification in real-time RT-PCR. Nucleic Acids Res. *29*, e45.

Price, A.L., Patterson, N.J., Plenge, R.M., Weinblatt, M.E., Shadick, N.A., and Reich, D. (2006). Principal components analysis corrects for stratification in genome-wide association studies. Nat Genet *38*, 904–909.

Pruitt, K.D., Tatusova, T., Brown, G.R., and Maglott, D.R. (2012). NCBI Reference Sequences (RefSeq): current status, new features and genome annotation policy. Nucleic Acids Res. *40*, D130–D135.

Roadmap Epigenomics Consortium, Kundaje, A., Meuleman, W., Ernst, J., Bilenky, M., Yen, A., Heravi-Moussavi, A., Kheradpour, P., Zhang, Z., Wang, J., et al. (2015). Integrative analysis of 111 reference human epigenomes. Nature *518*, 317–330.

Schizophrenia Working Group of the Psychiatric Genomics (2014). Biological insights from 108 schizophrenia-associated genetic loci. Nature *511*, 421–427.

Schmieder, R., and Edwards, R. (2011). Quality control and preprocessing of metagenomic datasets. Bioinformatics *27*, 863–864.

Sheehan, D.V., Lecrubier, Y., Sheehan, K.H., Amorim, P., Janavs, J., Weiller, E., Hergueta, T., Baker, R., and Dunbar, G.C. (1998). The Mini-International Neuropsychiatric Interview (M.I.N.I.): the development and validation of a structured diagnostic psychiatric interview for DSM-IV and ICD-10. J Clin Psychiatry *59 Suppl 20*, 22–33–quiz34–57.

Spijker, S. (2011). Dissection of Rodent Brain Regions. In Neuroproteomics, (Totowa, NJ: Humana Press), pp. 13–26.

Stahl, E.A., Raychaudhuri, S., Remmers, E.F., Xie, G., Eyre, S., Thomson, B.P., Li, Y., Kurreeman, F.A.S., Zhernakova, A., Hinks, A., et al. (2010). Genome-wide association study meta-analysis identifies seven new rheumatoid arthritis risk loci. Nat Genet *42*, 508–514.

Wagner, K.V., Hartmann, J., Mangold, K., Wang, X.-D., Labermaier, C., Liebl, C., Wolf, M., Gassen, N.C., Holsboer, F., Rein, T., et al. (2013). Homer1 mediates acute stress-induced cognitive deficits in the dorsal hippocampus. J. Neurosci. *33*, 3857–3864.

Wang, K., Li, M., and Hakonarson, H. (2010). ANNOVAR: functional annotation of genetic variants from high-throughput sequencing data. Nucleic Acids Res. *38*, e164.

Ward, L.D., and Kellis, M. (2012). HaploReg: a resource for exploring chromatin states, conservation, and regulatory motif alterations within sets of genetically linked variants. Nucleic Acids Res. *40*, D930–D934.

Wickham, H. (2009). ggplot2: Elegant Graphics for Data Analysis (Springer Publishing Company, Incorporated).

Zhang, Y., Liu, T., Meyer, C.A., Eeckhoute, J., Johnson, D.S., Bernstein, B.E., Nusbaum, C., Myers, R.M., Brown, M., Li, W., et al. (2008). Model-based analysis of ChIP-Seq (MACS). Genome Biol *9*, R137.

SUPPLEMENTAL NOTES

List of collaborators of the Major Depressive Disorder Working Group of the Psychiatric Genomics Consortium.

#	First name	Last name	Affiliation	#	First name	Last name	Affiliation
1	Stephan	Ripke	Harvard University/Broad Institute	59	Michel	Guipponi	University of Geneva
2	Naomi R	Wray	Queensland Institute of Medical Research/University of Queen	60	Anjali K	Henders	Queensland Institute of Medical Research
3	Cathryn M	Lewis	Institute of Psychiatry, King's College London	61	Stefan	Herms	University of Bonn
4	Steven P	Hamilton	University of California, San Francisco	62	Ian B	Hickie	University of Sydney, Sydney
5	Myrna M	Weissman	Columbia University	63	Susanne	Hoefels	University of Bonn
6	Gerome	Breen	Institute of Psychiatry, King's College London	64	Witte	Hoogendijk	Erasmus Medical Center
7	Enda M	Byrne	Queensland Institute of Medical Research	65	Jouke Jan	Hottenga	VU University, Amsterdam
8	Douglas HR	Blackwood	University of Edinburgh	66	Dan V	Iosifescu	Massachusetts General Hospital
9	Dorret I	Boomsma	VU University, Amsterdam	67	Marcus	Ising	Max Planck Institute of Psychiatry
10	Sven	Cichon	University of Bonn	68	Ian	Jones	Cardiff University
11	Andrew C	Heath	Washington University, St Louis	69	Lisa	Jones	University of Birmingham
12	Florian	Holsboer	Max Planck Institute of Psychiatry	70	Tzeng	Jung-Ying	North Carolina State University
13	Susanne	Lucae	Max Planck Institute of Psychiatry	71	James A	Knowles	University of Southern California
14	Pamela AF	Madden	Washington University, St Louis	72	Isaac S	Kohane	Brigham and Women's Hospital
15	Nicholas G	Martin	Queensland Institute of Medical Research	73	Martin A	Kohli	Max Planck Institute of Psychiatry
16	Peter	McGuffin	Institute of Psychiatry, King's College London	74	Ania	Korszun	Queen Mary University of London
17	Pierandrea	Muglia	GlaxoSmithKline	75	Mikael	Landen	Karolinska Institutet
18	Markus M	Noethen	University of Bonn	76	William B	Lawson	Howard University
19	Brenda P	Penninx	VU University Medical Center, Amsterdam	77	Glyn	Lewis	University of Bristol
20	Michele L	Pergadia	Washington University, St Louis	78	Donald	MacIntyre	University of Edinburgh
21	James B	Potash	University of Iowa	79	Wolfgang	Maier	University of Bonn
22	Marcella	Rietschel	Central Inst Mental Health, University of Heidelberg	80	Manuel	Mattheisen	University of Bonn
23	Danyu	Lin	University of North Carolina	81	Patrick J	McGrath	Columbia University
24	Bertram	Müller-Myhsok	Max Planck Institute of Psychiatry	82	Andrew	McIntosh	University of Edinburgh
25	Jianxin	Shi	National Cancer Institute	83	Alan	McLean	University of Edinburgh
26	Stacy	Steinberg	deCODE Genetics	84	Christel M	Middeldorp	VU University, Amsterdam
27	Hans J	Grabe	University of Greifswald	85	Lefkos	Middleton	Imperial College
28	Paul	Lichtenstein	Karolinska Institutet	86	Grant M	Montgomery	Queensland Institute of Medical Research
29	Patrik	Magnusson	Karolinska Institutet	87	Shawn N	Murphy	Massachusetts General Hospital
30	Roy H	Perlis	Massachusetts General Hospital	88	Matthias	Nauck	University of Greifswald
31	Martin	Preisig	University of Lausanne	89	Willem A	Nolen	Groningen University Medical Center
32	Jordan W	Smoller	Massachusetts General Hospital	90	Dale R	Nyholt	Queensland Institute of Medical Research
33	Kari	Stefansson	deCODE Genetics	91	Michael	O'Donovan	Cardiff University
34	Rudolf	Uher	Institute of Psychiatry, King's College London	92	Högni	Oskarsson	Therapeia, University Hospital
35	Zoltan	Kutalik	University of Lausanne	93	Nancy	Pedersen	Karolinska Institutet
36	Katherine E	Tansey	Institute of Psychiatry, King's College London	94	William A	Scheftner	Rush University Medical Center
37	Alexander	Teumer	University of Greifswald	95	Andrea	Schulz	University of Greifswald
38	Alexander	Viktorin	Karolinska Institutet	96	Thomas G	Schulze	University of Goettingen
39	Michael R	Barnes	GlaxoSmithKline	97	Stanley I	Shyn	University of Washington
40	Thomas	Bettecken	Max Planck Institute of Psychiatry	98	Engilbert	Sigurdsson	Landspitali University Hospital
41	Elisabeth B	Binder	Max Planck Institute of Psychiatry	99	Susan L	Slager	Mayo Clinic
42	René	Breuer	Central Inst Mental Health, University of Heidelberg	100	Johannes H	Smit	VU University Medical Center, Amsterdam
43	Victor M	Castro	Partners HealthCare System	101	Hreinn	Stefansson	deCODE Genetics
44	Susanne E	Churchill	Partners HealthCare System	102	Michael	Steffens	University of Bonn
45	William H	Coryell	University of Iowa	103	Thorgeir	Thorgeirsson	deCODE Genetics
46	Nick	Craddock	Cardiff University	104	Federica	Tozzi	GlaxoSmithKline
47	Ian W	Craig	Institute of Psychiatry, King's College London	105	Jens	Treutlein	Central Inst Mental Health, University of Heidelberg
48	Darina	Czamara	Max Planck Institute of Psychiatry	106	Manfred	Uhr	Max Planck Institute of Psychiatry
49	Eco J	De Geus	VU University, Amsterdam	107	Edwin JCG	van den Oord	Virginia Commonwealth University
50	Franziska	Degenhardt	University of Bonn	108	Gerard	Van Grootheest	VU University Medical Center, Amsterdam
51	Anne E	Farmer	Institute of Psychiatry, King's College London	109	Henry	Völzke	University of Greifswald
52	Maurizio	Fava	Massachusetts General Hospital	110	Jeffrey B	Weilburg	Massachusetts General Hospital
53	Josef	Frank	Central Inst Mental Health, University of Heidelberg	111	Gonneke	Willemsen	VU University, Amsterdam
54	Vivian S	Gainer	Partners HealthCare System	112	Frans G	Zitman	Leiden University Medical Center, Leiden
55	Patience J	Gallagher	Massachusetts General Hospital	113	Benjamin	Neale	Harvard University/Broad Institute
56	Scott D	Gordon	Queensland Institute of Medical Research	114	Mark	Daly	Harvard University/Broad Institute
57	Sergey	Goryachev	Partners HealthCare System	115	Douglas F	Levinson	Stanford University
58	Magdalena	Gross	University of Bonn	116	Patrick F	Sullivan	University of North Carolina